

International Journal of Applied Sciences and Smart Technologies

Volume 01, Issue 02, December 2019

Measuring Privacy Leakage in Term of Shannon Entropy

Ricky Aditya, Boris Skoric

On the Synthesis of a Linear Quadratic Controller for a Quadcopter

Hendra G. Harno

Development of Stamping Machine Module to Improve Practical Competency

Pippie Arbiyanti

**Saving the Moving Position on the Continuous Passive Motion Machine for
Rehabilitation of Shoulder Joints**

Antonius Hendro Noviyanto

**Microcontroller Based Simple Water Flow Rate Control System to Increase
the Efficiency of Solar Energy Water Distillation**

Elang Parikesit, Wibowo Kusbandono, FA. Rusdi Sambada

**Morphological Map Analysis in Design Cashew Sheller (Kacip) as a Creative
Process to Produce Design Concept**

Bertha Bintari Wahyujati

**Design and Development of a Path-Tracking System Based on Radio
Frequency Identification Sensor for Educational Toy Robot (EDOT)**

Martinus Bagus Wicaksono

**Designing Independent Automatic Drinking Water Platforms at
Sanata Dharma University**

Muhammad Prayadi Sulistyanto, Ervan Erry Pramesta

p-ISSN 2655-8564 & e-ISSN 2685-9432

CONTENTS

CONTENTS	i
EDITORIAL BOARD	ii
PREFACE	iii
Measuring Privacy Leakage in Term of Shannon Entropy <i>Ricky Aditya, Boris Skoric</i>	85–100
On the Synthesis of a Linear Quadratic Controller for a Quadcopter <i>Hendra G. Harno</i>	101–112
Development of Stamping Machine Module to Improve Practical Competency <i>Pippie Arbiyanti</i>	113–120
Saving the Moving Position on the Continuous Passive Motion Machine for Rehabilitation of Shoulder Joints <i>Antonius Hendro Noviyanto</i>	121–128
Microcontroller Based Simple Water Flow Rate Control System to Increase the Efficiency of Solar Energy Water Distillation <i>Elang Parikesit, Wibowo Kusbandono, FA. Rusdi Sambada</i>	129–146
Morphological Map Analysis in Design Cashew Sheller (<i>Kacip</i>) as a Creative Process to Produce Design Concept <i>Bertha Bintari Wahyujati</i>	147–168
Design and Development of a Path-Tracking System Based on Radio Frequency Identification Sensor for Educational Toy Robot (EDOT) <i>Martinus Bagus Wicaksono</i>	169–178
Designing Independent Automatic Drinking Water Platforms at Sanata Dharma University <i>Muhammad Prayadi Sulistyanto, Ervan Erry Pramesta</i>	179–188
AUTHOR GUIDELINES	189

EDITORIAL BOARD

Editor in Chief

Dr. I Made Wicaksana Ekaputra (*Sanata Dharma University, Yogyakarta, Indonesia*)

Email: *made@usd.ac.id*

Associate Editor

Dr. Pham Nhu Viet Ha (*Vietnam Atomic Energy Institute, Hanoi, Vietnam*)

Dr. Hendra Gunawan Harno (*Gyeongsang National University, Jinju, The Republic of Korea*)

Dr. Iswanjono (*Sanata Dharma University, Yogyakarta, Indonesia*)

Dr. Mukesh Jewariya (*National Physical Laboratory, New Delhi, India*)

Dr. Mongkolserj Lin (*Institute of Technology of Cambodia, Phnom Penh, Cambodia*)

Dr. Yohanes Baptista Lukiyanto (*Sanata Dharma University, Yogyakarta, Indonesia*)

Dr. Apichate Maneewong (*Thailand Institute of Nuclear Technology, Bangkok, Thailand*)

Dr. Sudi Mungkasi (*Sanata Dharma University, Yogyakarta, Indonesia*)

Dr. Pranowo (*Universitas Atma Jaya Yogyakarta, Yogyakarta, Indonesia*)

Dr. Mahardhika Pratama (*Nanyang Technological University, Singapore*)

Dr. Augustinus Bayu Primawan (*Sanata Dharma University, Yogyakarta, Indonesia*)

Prof. Dr. Leo Hari Wiryanto (*Bandung Institute of Technology, Bandung, Indonesia*)

Editorial Proofreader

Ir. Ignatius Aris Dwiatmoko, M.Sc. (*Sanata Dharma University, Yogyakarta, Indonesia*)

P. H. Prima Rosa, S.Si., M.Sc. (*Sanata Dharma University, Yogyakarta, Indonesia*)

Editorial Assistant

Eduardus Hardika Sandy Atmaja, M.Cs. (*Sanata Dharma University, Yogyakarta, Indonesia*)

Vittalis Ayu, M.Cs. (*Sanata Dharma University, Yogyakarta, Indonesia*)

Administration

Catharina Maria Sri Wijayanti, S.Pd. (*Sanata Dharma University, Yogyakarta, Indonesia*)

Contact us

International Journal of Applied Sciences and Smart Technologies

Faculty of Science and Technology

Sanata Dharma University

Kampus III Paingan, Maguwoharjo, Depok, Sleman

Yogyakarta, 55282

Phone : +62 274883037 ext. 523110, 52320

Fax : +62 272886529

Email : editorial.ijasst@usd.ac.id

Website : <http://e-journal.usd.ac.id/index.php/IJASST>

IJASST is an open-access peer-reviewed journal that mediates the dissemination of research and studies conducted by academicians, researchers, and practitioners in science, engineering, and technology.

PREFACE

It is a great challenge to bring *International Journal of Applied Sciences and Smart Technologies* (IJASST) into international community, primarily when the journal aims to publish high-quality manuscripts. This journal aims to give readers worldwide with high quality peer-reviewed scholarly articles on a wide variety of issues related to technology, such as applied mathematics, physics, and chemistry. We are honored to announce that finally, we have finished processing volume one issue two of IJASST for the edition of December 2019.

This volume includes eight manuscripts from different institutions and subjects related to applied sciences and smart technologies. We always try to keep the quality of every published volume and issue by selecting the received manuscripts. All manuscripts follow the peer-reviewed procedure and will be reviewed using the open journal system (OJS) of IJASST. We believe that all the papers published in this issue will have a significant influence on this journal's scope.

We want to thank all who kindly contributed their papers for this issue and the editors of IJASST for their kind help and co-operation. For future issues, we are looking forward to your submissions to IJASST.

Dr. I Made Wicaksana Ekaputra
Editor in Chief
IJASST

This page intentionally left blank

Measuring Privacy Leakage in Term of Shannon Entropy

Ricky Aditya^{1,*}, Boris Skoric²

¹*Department of Mathematics, Faculty of Science and Technology,
Sanata Dharma University, Yogyakarta, Indonesia*

²*Security Group, Eindhoven University of Technology, Eindhoven,
The Netherlands*

**Corresponding Author: y_ricky_aditya@yahoo.com*

(Received 17-05-2019; Revised 28-06-2019; Accepted 31-07-2019)

Abstract

Differential privacy is a privacy scheme in which a database is modified such that each user's personal data are protected without affecting significantly the characteristics of the whole data. Example of such mechanism is Randomized Aggregatable Privacy-Preserving Ordinal Response (RAPPOR). Later it is found that the interpretations of privacy, accuracy and utility parameters in differential privacy are not totally clear. Therefore in this article an alternative definition of privacy aspect are proposed, where they are measured in term of Shannon entropy. Here Shannon entropy can be interpreted as number of binary questions an aggregator needs to ask in order to learn information from a modified database. Then privacy leakage of a differentially private mechanism is defined as mutual information between original distribution of an attribute in a database and its modified version. Furthermore, some simulations using the MATLAB software for special cases in RAPPOR are also presented to show that this alternative definition does make sense.

Keywords: differential privacy, RAPPOR, Shannon entropy, mutual information, privacy leakage.

1 Introduction

In digitalized era when many things can be done online, privacy becomes a more serious issue, especially if our personal data have to be submitted online for some reasons. Even with their published privacy policies (something that most users never read it properly), there are some room for privacy violations. Here we will not talk about the hackers or any outsiders, because the ones who violate privacy might come from the authorized parties.

The most annoying case is when some parties use their authorities to leak someone's private data but there is no laws or rules which can conclude it as a privacy violation and therefore they cannot be punished. For example, our medical record data which are recorded in a hospital's database. Our data, together with other persons' data, might be used by other parties who want to learn something from the database, let us say a medicine company or a medical research center. We never know if they really just access the database for gaining only the necessary information, or they may search for our personal data.

A basic and simplest way to prevent this is by hiding the names of data owners, i.e. making the data to be anonymous. Unfortunately, this may be not enough to protect our private data. They can still access any other data, such as height, weight, age, gender, etc. Consider some persons with a very rare attribute, for examples : too tall, too short, too fat, too thin, and many more. By looking at one specific attribute or two, they can uniquely determine them and as consequence, can leak their private information. They, of course, violate those persons' privacy but we cannot say that they break any laws or rules in the privacy policies. Suppose that someone is famous as the tallest guy in his/her city. Roughly saying, as long as they do not ask the hospital who the tallest guy in this database is, and the hospital do not inform it either, no laws or rules are broken.

Based on this kind of issues, many data security researchers try to create a new privacy protocol to protect any private information. One of them is called as differential privacy. The idea is to modify the original database such that each user's personal data

are protected but characteristics of the whole database do not change significantly. Therefore other parties are still able to learn any information about the whole database but they are unable to learn any personal information.

As a very simple example, there are five persons : A, B, C, D and E. The fact is A and B are smokers, while the others not. After modification, the smokers become C and E. Here the fact that A and B are smokers is hidden, but it preserves the fact that two of those five persons are smokers. Note that other parties know that the database has been modified, so they cannot judge C and E as smokers. Therefore if they just want to know the proportion of smokers in the database, they will not get it wrong but they will not know who the real smokers are.

In practical case, of course, we will work on much larger database with various attributes. We do not have to preserve the exact proportion of any attributes, but we need to keep it with a small margin of errors. The concept of differential privacy will be discussed in the next section, together with some specific mechanisms which can be used.

2 Differential Privacy and RAPPOR

The idea of differential privacy came first in Dwork et.al. [1] in 2006. In their work, an idea to protect privacy by adding noise to the data is introduced. At that time, it had not been named as differential privacy, the name came later after some subsequent research. After few years working thoroughly on this area, a more comprehensive concept of differential privacy are later published in Dwork and Roth [2]. Concepts and definitions in this section are based on [1] and [2].

2.1 Differential Privacy

Now we go to the definition of differential privacy. Let a database is represented in a table in which the rows represent the users and the columns represent the attributes. Sometimes the parties who have authorized access to the database only need to take some samples of users and not all of them. We do not always know what they want to look for, but we can assume that they have full authorities to do so.

We say that two sub-databases are neighboring to each other if one is obtained by adding or deleting one row from the other. If the database is not modified, it is possible to learn about one specific user by learning two databases : one database that containing him/her and the database that is obtained by eliminating him/her from the previous one. Therefore, in order to protect that user's privacy the modification mechanism needs to eliminate this possibility. This leads to a definition of differentially private mechanism.

Definition 2.1. *Let A be a mechanism to modify a database D with D' as output. The mechanism A is said to be (ϵ, δ) -differentially private, where both ϵ and δ are non-negative numbers, if for any neighboring sub-databases x_1 and x_2 of D , and for any subset S of D' , it satisfies :*

$$\Pr[A(x_1) \in S] \leq e^\epsilon \cdot \Pr[A(x_2) \in S] + \delta \quad (1)$$

Equation (1) can be interpreted as the outputs from two neighboring databases has only very small and insignificant difference such that (almost) nothing can be learned about the user who differs them. If the numbers ϵ dan δ be smaller, then the differences become more insignificant and the privacy becomes stronger. In some specific cases, the parameter δ in (1) is set to be 0 and then the mechanism is said to be ϵ - differentially private.

Now we talk about the accuracy of a differential privacy mechanism. In this context we are concerned about information from a database which can be used to answer predicate counting queries. The class of those queries is called as concept class, usually denoted by C . Set of any possible values of a database is called as data universe, usually denoted by X . Output of a predicate counting query c on a database x , denoted by $c(x)$, is the proportion of elements in x which satisfy that predicate. For example, proportion of smokers or proportion of patients with heart problem in a medical record database. Then we have this definition of accuracy.

Definition 2.2. *For any $c \in C$, a mechanism A on database x is said to be α -accurate for c if $|c(x) - c(A(x))| < \alpha$. Moreover, A is said to be (α, γ) -accurate for a concept class C if A is α -accurate for $(1-\gamma)$ fractions of queries in C .*

Above definition can be interpreted as even though each personal data has been modified, but the proportion of users who satisfy a predicate does not change significantly. We need α to be smaller for a better accuracy. Considering that it is very difficult to create a mechanism that can be accurate for all queries in a concept class, then parameter γ is introduced. If γ is smaller, then more queries can be answered accurately. Furthermore, an utility parameter of a mechanism can also be defined based on its accuracy parameter.

Definition 2.3. *Let C be a concept class and X is a data universe. A modification mechanism A is said to have (α, β, γ) -utility with respect to C and X if for a database x it holds that $\Pr[A \text{ is } (\alpha, \gamma)\text{-accurate}] \leq \beta$.*

There are several kind of mechanisms which can be used to modify database which satisfy differential privacy principles. In this section we will introduce the Randomized Aggregatable Privacy-Preserving Ordinal Response (RAPPOR) mechanism. The next sub-section will discuss more about RAPPOR.

2.2 Randomized Aggregatable Privacy-Preserving Ordinal Response (RAPPOR)

Let a database consists of several attributes which each of them can be divided into several categories. For example, we can categorize people according to their genders (male/female), age range ($\leq 20, 21 - 40, 41 - 60, \geq 60$) and many more. Then for each attribute, each user is represented as the category he/she belongs to. To represent in which category a user belongs to, we can also use as a binary vector with exactly one 1 and 0 otherwise, where position of the 1 denotes the category he/she belongs to.

These binary vector representations will then be modified randomly based on a probability distribution and sent to other parties. Thus they will receive an already modified database. To learn about distribution of categories for each attribute, they have to take the aggregate values of each category. Because of this, later we will call them as data aggregator. The data aggregator does not know the actual distribution of categories, but he/she may know the probability distribution that is used to modify the database.

However, this knowledge should not be enough to leak actual information of the entire database.

There are several kind of RAPPOR mechanisms, as presented in Wang et.al. [3]. In this article we will discuss two kind of RAPPOR mechanisms, which are

1. RAPPOR with direct representation

This kind of data aggregation mechanism works as follows Let there are m categories in an attribute and a user i belongs to category C_i' . After modification, user i belongs to category C_i' . Probability that user i still in his/her actual category ($C_i = C_i'$) is γ and for each category j where $j \neq C_i'$, probability of user i belongs to category j after modification is $\gamma/(m - 1)$.

2. RAPPOR with unary representation.

In this mechanism, category of a user i is represented as a binary vector $X_i = (X_{i1}, X_{i2}, \dots, X_{im})$ where $X_{ij} = 1$ if user i belongs to category j and otherwise $X_{ij} = 0$. Then this binary vector will be modified by adding noise independently on each bit. Here a bit 0 can be flipped to 1 or vice versa. For each bit, probability of binary flip from 0 to 1 is β_0 and probability of binary flip from 1 to 0 is β_1 . If $\beta_0 = \beta_1$, then it is called as symmetric scheme. The modified vector is then denoted as Z_i and this will be sent to the aggregator. Note that after modification, it is possible to have more than one 1s or no 1s at all.

In next sections, we will not discuss the privacy and accuracy aspects using Definition 2.1. and Definition 2.2., but we will use a different approach instead, that is, by using concepts from information theory and we will see how it could work.

3 Re-defining Privacy Leakage in Term of Shannon

Entropy

There are some open problems from the concepts of differential privacy explained in the previous section. For example, in a differentially private scheme, we want to determine the values of ϵ and δ such that its privacy can be considered as good enough and the values of α , β and γ such that it has good accuracy and/or utility. We are also

interested in the practical interpretation of those parameters in a specific mechanism and how changes of one or two parameters affect the others.

It is difficult to answer those questions since we do not have a well-defined measurements of some parameters in differential privacy. Thus we might need another way of measuring the strength of privacy and accuracy. In Wang et.al. [4], an idea that linked differential privacy and mutual-information privacy was introduced. Therefore it should be possible to learn differential privacy using information theoretic approach. In this section we will use similar idea to re-define some aspects of differential privacy in the language of information theory.

3.1 Shannon Entropy and Mutual Information

Intuitively, stronger privacy will imply worse accuracy and vice versa. As a consequence, we cannot have both aspects at each highest level and we should try to find a solution for “optimizing” both privacy and accuracy. Therefore their measurements have to be “sensibly comparable”. In this section an alternative definition for privacy aspect in differential privacy based on information theory point of view will be introduced. Some basic definitions in information theory, based on Cover and Thomas [5], will be revisited first.

Definition 3.1. *Let X be a random variable with probability distribution P and probability mass function $p_x = \Pr[X = x]$. Shannon entropy of X , denoted by $H(X)$, is defined as :*

$$H(X) = E[-\log(p_x)] = \sum_{x \in X} p_x \cdot \log\left(\frac{1}{p_x}\right). \quad (2)$$

Binary entropy function h of an event with probability p is defined as :

$$h(p) = p \cdot \log\left(\frac{1}{p}\right) + (1-p) \cdot \log\left(\frac{1}{1-p}\right). \quad (3)$$

In some books, Shannon entropy is often called just by the word “entropy”. There are many interpretations of Shannon entropy. One of them is the number of binary (yes/no) questions which need to be asked in order to learn an output if the probability

distribution is known. This interpretation might be not totally accurate, but it is sensible enough to define privacy aspect. If the aggregator needs to ask too many questions in order to learn about an individual data, then we can say that the privacy is strong enough.

After being modified, a database might still give some partial information about its actual data. By learning an already modified database, an aggregator might be able to leak some actual information without knowing the original one. This “leakage” can be represented as mutual information between an original database and its modified version. The following is the definition of mutual information.

Definition 3.2. *Let X and Y be two random probability distributions. Mutual information between X and Y , denoted by $I(X;Y)$, can be computed using these equivalent formulas:*

$$\begin{aligned} I(X;Y) &= H(X) - H(X|Y) = H(Y) - H(Y|X) \\ &= H(X) + H(Y) - H(XY) = H(XY) - H(X|Y) - H(Y|X) \end{aligned} \quad (4)$$

Moreover, if X and Y have joint probability distribution p_{xy} and their respective marginal probability mass functions are $p_x = \sum_y p_{xy}$ and $p_y = \sum_x p_{xy}$, then :

$$I(X;Y) = \sum_{x,y} p_{xy} \cdot \log \left(\frac{p_{xy}}{p_x \cdot p_y} \right) \quad (5)$$

Based on Shannon entropy and mutual information as in Definition 3.1. and 3.2., we can create new definitions of privacy aspect of differential privacy. These will be discussed in next sub-section.

3.2 Alternative Definitions of Privacy Leakage

If we go to our implementation, then we can directly get an idea to define a privacy leakage. Suppose that C is the actual distribution of an attribute in a database and after modification the distribution becomes C' . The privacy leakage can be defined as mutual information between C and C' , i.e. $I(C;C')$, which can be interpreted as the number of binary questions asked by an aggregator to learn information about actual distribution C that can be answered by his/her knowledge on modified distribution C' . By this

interpretation, a stronger privacy scheme should have smaller value of mutual information between actual distribution and modified distribution.

Meanwhile, defining accuracy and utility are trickier. If we want to make everything well-defined, then we need a sensible interpretation about utility in term of the number of binary questions. This is for making a comparable measure between privacy and accuracy-utility. If one entropy in privacy has different interpretation with one entropy in accuracy/utility, then these measures are incomparable and we will not get what we expect in the beginning. This can be an open problem for any possible further research. In next section we are going to do some simulations using the MATLAB software to justify whether our definitions of privacy leakage and utility really make sense or not.

4 Simulation using the MATLAB Software

Alternative definition of privacy leakage introduced in previous section look make sense, but sometimes we need to justify them using some simulations in real and practical cases. Here we do simulations on privacy leakage first. Since computation of a big enough database would take long enough time to compute, we start with some special cases in small database which their computations do not take much time to complete.

4.1 Case I : RAPPOR with direct representation

Recall the mechanism of RAPPOR with direct representation introduced in Section 2. In this mechanism, a user which belongs to a category will have probability $1 - \gamma$ to stay in his/her actual category and probability $\gamma/(m - 1)$ to move into each of other categories, where m denotes the number of categories. Therefore if we know the actual distribution C , we can compute the entropy of conditional probability distribution $C'|C$ as below

$$\begin{aligned} H(C'|C) &= H\left(\left(1-\gamma, \frac{\gamma}{m-1}, \dots, \frac{\gamma}{m-1}\right)\right) = (1-\gamma) \cdot \log \frac{1}{1-\gamma} + (m-1) \cdot \left[\frac{\gamma}{m-1} \cdot \log \left(\frac{m-1}{\gamma}\right) \right] \\ &= (1-\gamma) \cdot \log \frac{1}{1-\gamma} + \gamma \cdot \left[\log(m-1) + \log \frac{1}{\gamma} \right] = (1-\gamma) \cdot \log \frac{1}{1-\gamma} + \gamma \cdot \log \frac{1}{\gamma} + \gamma \cdot \log(m-1) \end{aligned}$$

$$= h(\gamma) + \gamma \cdot \log(m-1) \tag{6}$$

Now we want to compute entropy of modified distribution C' . Let the actual distribution be (p_1, p_2, \dots, p_m) . We will determine the probability that a user would end up in category j , no matter what his/her actual category is. Let denote that probability as r_j . If a user is originally in category j (with probability p_j), then his/her probability to stay in category j is $(1 - \gamma) \cdot p_j$. If he/she is originally in another category i (with probability $p_i, i \neq j$), then his/her probability to move to category j is $(\gamma \cdot p_i)/(m - 1)$. Taking sum of these disjoint cases, we get a formula of r_j that is

$$r_j = (1-\gamma) \cdot p_j + \sum_{\substack{i=1 \\ i \neq j}}^m \left(\frac{\gamma}{m-1} \right) \cdot p_i = (1-\gamma) \cdot p_j + \left(\frac{\gamma}{m-1} \right) \cdot (1-p_j) = \frac{\gamma}{m-1} + \left(1 - \frac{\gamma m}{m-1} \right) \cdot p_j \tag{7}$$

Thus distribution of C' is (r_1, r_2, \dots, r_m) , and mutual information between C and C' is

$$I(C'; C) = H(C') - H(C'|C) = \sum_{i=1}^m r_j \cdot \log \frac{1}{r_j} - h(\gamma) - \gamma \cdot \log(m-1) \tag{8}$$

where r_j is as defined in (7). This is the measurement of privacy leakage in this mechanism with probability parameter γ .

After obtaining formula (8), we can try to do a computation of it. To simplify the computation, we try on a special case where the actual distribution is uniform, i.e. the users are distributed uniformly into m categories with probability $1/m$ each. In this case we will have :

$$r_j = \frac{\gamma}{m-1} + \left(1 - \frac{\gamma m}{m-1} \right) \cdot p_j = \frac{\gamma}{m-1} + \left(1 - \frac{\gamma m}{m-1} \right) \cdot \frac{1}{m} = \frac{\gamma}{m-1} + \frac{1}{m} - \frac{\gamma}{m-1} = \frac{1}{m}$$

$$I(C'; C) = \sum_{i=1}^m r_j \cdot \log \frac{1}{r_j} - h(\gamma) - \gamma \cdot \log(m-1)$$

$$= \sum_{i=1}^m \frac{1}{m} \cdot \log m - h(\gamma) - \gamma \cdot \log(m-1) = \log m - h(\gamma) - \gamma \cdot \log(m-1) \tag{9}$$

Now we compute formula (9) of variable γ . We consider several cases with different number of categories 2, 3, 4 and 5 categories. Results of these computations are shown in Figure 1.

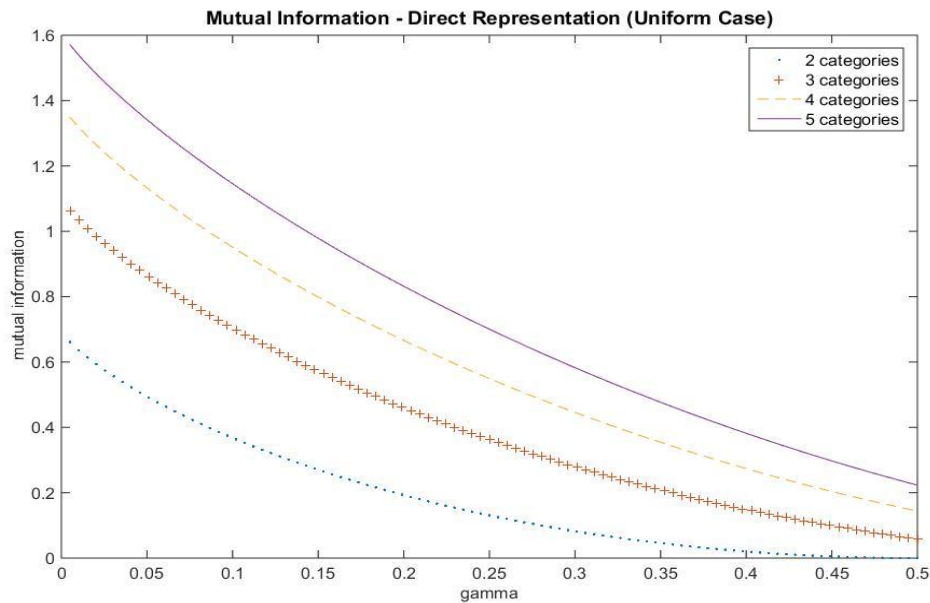


Figure 1. Privacy leakage of RAPPOR with direct representation. Graphs of mutual information $I(C'; C)$ as a function of the noise parameter γ are plotted for $m = 2, 3, 4$ and 5 , where the actual distribution C is uniform.

We can see the behavior of those graph. When γ is closer to 0.5 , the mutual information is closer to 0 and therefore get stronger privacy. We also see that if there are more categories, the value of mutual information is also bigger. However, we have not been able to compare multiple cases with different number of categories. Look at the fact that formula (9) depends on the value of m and if m is bigger, then $I(C'; C)$ shall be bigger too. This leads to a possible kind of “normalization”, which makes the value of mutual information fall in interval $[0,1]$. If $\gamma = 0$, the “normalized” mutual information should be equal to 1 , which means that the aggregator is fully able to learn any information in the database since he/she receives the original one. Unfortunately we are yet to find a formulation about the normalization factor.

4.2 Case II : RAPPOR with unary representation

Now we move on to another case of RAPPOR with unary representation. To simplify the case, we will consider the symmetric case when $\beta_0 = \beta_1$ (to avoid many subscripts, later they are both written as β). Each user can only belong to one category and

therefore his/her binary vector representation C contains exactly one 1 in his/her category's position and 0 otherwise. Given an arbitrary binary m -vector z , we will compute the probability that the binary vector representation will be modified into z . This shall depend on how many 1s are contained in z , i.e. the Hamming weight of z , usually denoted by $w(z)$.

If the 1 in original vector C is not flipped to 0, then from $m - 1$ 0s in C , there are $w(z) - 1$ of them which are flipped into 1 and the other $m - w(z)$ 0s are not flipped. Its probability will be $\beta^{w(z)-1} (1 - \beta)^{m - w(z)+1}$. In other side, if the 1 in C is flipped to 0, then from $m - 1$ 0s in C , there are $w(z)$ of them which are flipped into 1 and the other $m - w(z) - 1$ 0s are not flipped. Its probability will be $\beta^{w(z)+1} (1 - \beta)^{m - w(z)-1}$. As a result, the probability distribution Z of a modified database, knowing that a user belongs to category j , can be written as :

$$\Pr[Z = z | C = j] = \left(\frac{1 - \beta}{\beta}\right)^{2z_j} \beta^{w(z)+1} (1 - \beta)^{m - w(z)-1} \quad (10)$$

It looks like a tricky task to compute the entropy $H(Z|C)$ since we have to take sum from any possible binary vectors z with various Hamming weights and positions of their 1s. However, by using some binomial properties in Rosen [6], we can obtain a pretty simple result below :

$$H(Z|C) = m \cdot h(\beta) = m \left(\beta \log \frac{1}{\beta} + (1 - \beta) \log \frac{1}{1 - \beta} \right) \quad (11)$$

Defining $\Pr[Z = z]$, for any m -binary vector, is a lot more difficult. We have to consider any possible original position of the single 1, multiply it by its actual probability and take sum of them. Based on (10) we can compute that probability mass function, denoted by $Q(z)$, as :

$$\begin{aligned} Q(z) &= \Pr[Z = z] = \sum_{j=1}^m p_j \cdot \Pr[Z = z | C = j] \\ &= \sum_{j=1}^m p_j \left(\frac{1 - \beta}{\beta}\right)^{2z_j} \beta^{w(z)+1} (1 - \beta)^{m - w(z)-1} \end{aligned}$$

$$= \left(\frac{\beta}{1-\beta} \right)^{w(z)} \beta(1-\beta)^{m-1} \sum_{j=1}^m p_j \left(\frac{1-\beta}{\beta} \right)^{2z_j} \quad (12)$$

Note that values of z_j are either 0 or 1, so we can divide the last sigma form in (12) into two cases when $z_j = 0$ and when $z_j = 1$. If we define $p(z) = \sum_j p_j \cdot z_j$, then (12) can be simplified into

$$\begin{aligned} Q(z) &= \left(\frac{\beta}{1-\beta} \right)^{w(z)} \beta(1-\beta)^{m-1} \left[\sum_{\substack{j=1 \\ z_j=1}}^m p_j \left(\frac{1-\beta}{\beta} \right)^2 + \sum_{\substack{j=1 \\ z_j=0}}^m p_j \left(\frac{1-\beta}{\beta} \right)^0 \right] \\ &= \left(\frac{\beta}{1-\beta} \right)^{w(z)} \beta(1-\beta)^{m-1} \left[p(z) \left(\frac{1-\beta}{\beta} \right)^2 + 1 - p(z) \right] \\ &= \left(\frac{\beta}{1-\beta} \right)^{w(z)} \beta(1-\beta)^{m-1} \left[1 + p(z) \frac{1-2\beta}{\beta^2} \right] \end{aligned} \quad (13)$$

Since entropy calculation involves logarithm and nothing can be simplified from logarithm of a sum, it will be difficult to simplify the $H(Z)$ term in this case. Therefore we try to do a “brute force” for calculating mutual information $I(Z; C) = H(Z) - H(Z|C)$ by directly using the last row of (13) in calculating $H(Z)$ term. Again we set the actual distribution of categories to be uniform and we compute multiple cases of different number of categories : 2, 3, 4 and 5 categories. Results of these computations are shown in Figure 2.

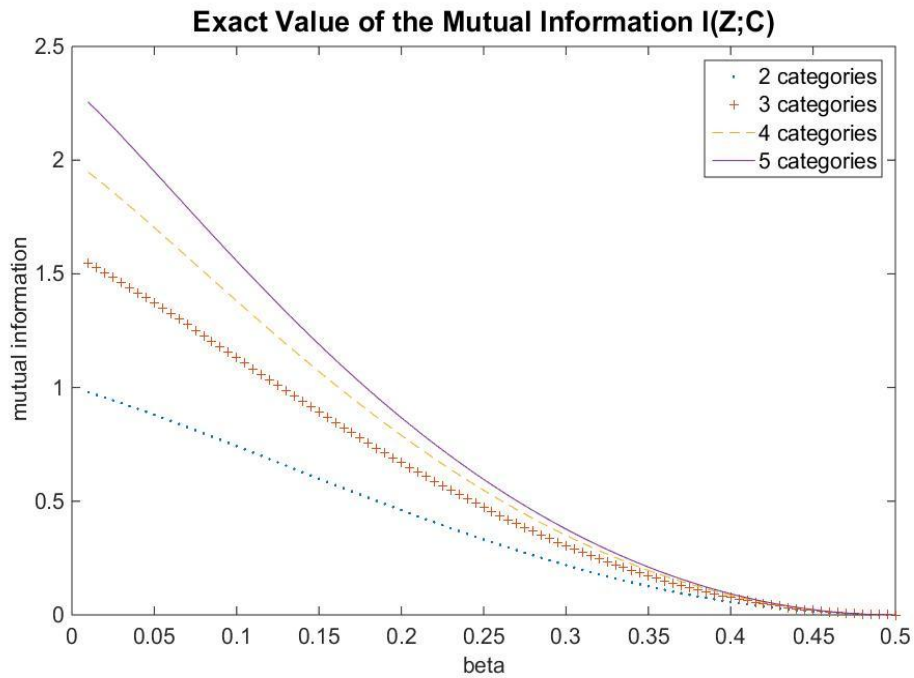


Figure 2. Privacy leakage of RAPPOR with unary representation. Graphs of mutual information $I(Z'; C)$ as a function of the noise parameter β are plotted for $m = 2, 3, 4$ and 5 , where the actual distribution C is uniform.

We see similar behavior with previous case. For any number of categories, their graphs are monotonically decreasing on interval $[0, 0.5]$. The difference is that all graphs tend to 0 when $\beta = 0.5$. We can interpret this as the aggregator is unable to learn anything when $\beta = 0.5$, i.e. the binary flip is totally random. More categories also imply bigger value of mutual information, but they are also yet to be normalized. Also note that if the range of β is extended to $[0, 1]$, then those graph will be monotonically increasing. Let us imagine if $\beta = 1$, then all binary vectors will be completely flipped (0 to 1 or vice versa) and the aggregator can easily determine the original ones. We can also intuitively conclude that cases when $\beta = t$ and $\beta = 1 - t$ are practically similar.

Apart from those two presented cases, we have tried to do computation for other mechanisms, but some of them have very complicated formula and be very difficult to compute. Some computations even need several days to be completed. Computation for a big enough number of categories is also yet to be done. There are two possible

solutions simplifying the computation, or determining upper/lower bound of the privacy leakage which is easier to compute.

5 Conclusions

From what are discussed in this article, we have several points of conclusions and feedbacks for any possible further research, which are :

1. By interpreting entropies as number of binary questions which are need to asked for learning information on a database, it is possible to re-define privacy and accuracy-utility aspects of a differential privacy scheme in term of entropies. In this article the former has been done.
2. Privacy leakage of a differentially private mechanism can be defined as the mutual information between actual distribution of categories of an attribute in a database and its modified version. This definition does make sense and some simulations with MATLAB have been done to justify it.
3. Defining accuracy and utility of a differentially private mechanism in term of entropies is a trickier task to do. One entropy in the definition of utility should have similar and comparable interpretation with one entropy in privacy leakage. This may still be very open problem.
4. Definitions of privacy leakage here is still lack of “normalization”. To make it totally comparable between any attributes with various number of categories, we might need to normalize them into a specific range (possibly $[0,1]$) and their normalization factors are yet to be determined. These could be some open problems to solve in further research.

Acknowledgements

This is a part of our work in the “Bridging the Gap between Theory and Practice in Data Privacy” (BRIDGE) project at Technische Universiteit Eindhoven in 2017, funded by the Netherlands Organization for Scientific Research (NWO) and National Science Foundation (NSF). This project should lead to a PhD degree in which initially the first

author was the PhD candidate. However, after several months the first author decided not to continue working on this project.

References

- [1] C. Dwork, F. McSherry, K. Nissim, and A. Smith, “Calibrating noise to sensitivity in private data analysis,” *Theory of Cryptography Conference*, New York, USA, 265–284, 2006.
- [2] C. Dwork and A. Roth, “The algorithmic foundations of differential privacy,” *Foundations and Trends in Theoretical Computer Science*, **9** (3–4), 211–407, 2014.
- [3] T. Wang, J. Blocki, N. Li, and S. Jha, “Locally differentially private protocols for frequency estimation,” *USENIX Security Symposium, Vancouver, British Columbia, Canada*, 729–745, 2017.
- [4] W. Wang, L. Ying, and J. Zhang, “On the relation between identifiability, differential privacy and mutual information privacy,” *IEEE Transactions on Information Theory*, **62** (9), 5018–5029, 2016.
- [5] T. M. Cover and J. A. Thomas, *Elements of Information Theory*, Second Ed, John Wiley & Sons Publication, Hoboken, USA, 2006.
- [6] K. H. Rosen, *Discrete Mathematics and Its Applications*, Seventh Ed, Mc Graw-Hill Education, New York, USA, 2011.

On the Synthesis of a Linear Quadratic Controller for a Quadcopter

Hendra G. Harno

*Department of Aerospace and Software Engineering,
Gyeongsang National University, Jinju 52828, Republic of Korea
Corresponding Author: h.g.harno@gmail.com*

(Received 31-05-2019; Revised 17-10-2019; Accepted 17-10-2019)

Abstract

This paper discusses about synthesizing a state-feedback controller for a quad copter based on an optimal linear quadratic control method. The resulting light control system enables the quad copter to maintain stability and to track a reference input. The solution to this control problem involves solving an algebraic Riccati equation. The reference-input tracking capability is simulated to show the capability of the quadcopter flight control system.

Keywords: flight control, quadcopter, linear quadratic control, tracking.

1 Introduction

Versatility of a quad copter has been celebrated by different communities, including, but not limited to, hobbyists, entrepreneurs, medical officers, defence forces, engineers and scientists. It has been used for various purposes (both civilian and military) that can benefit from the quadcopter as a flying vehicle. This is realizable because the quad copter is relatively easier to operate as compared to a full-scale conventional rotorcraft. Moreover, users also do not need a runway, an airport or a helipad to operate the quadcopter. In some applications, the quadcopter can even be controlled remotely in a

cost-effective manner to accomplish particular missions. It is also true that the quadcopter has a relatively simple design with an uncomplicated structure. Thus, operational and maintenance costs pertaining to quadcopter operations tend to be low. All these features have indeed signify the merit of the quadcopter for a wider usage nowadays and in the future [1, 2].

These advantages will be more meaningful for the users if the quadcopter carrying payloads is equipped with appropriate flight control, instrumentation and communication systems. The flight control system has particularly served as an indispensable part that enables the quadcopter to perform various maneuvers in its operation [3]. Thus, we will only discuss about synthesizing a linear controller to enable the quadcopter to fly properly. There are different sorts of control methods that can be applied to develop the flight control system such as PID control, H_2 or linear quadratic control, H_∞ control, sliding mode control and adaptive control (see e.g. [4, 5, 6]).

To construct the linear controller for the quadcopter, a linear time-invariant state space model is used to represent the quadcopter dynamics at a chosen trim condition (equilibrium point). In this case, the linear model was derived through the Taylor series expansion as presented in [7]. Parameters of this model were identified and validated based on the comprehensive identification from frequency responses (CIFER) method [8]. This system identification method is well known as one that is able to yield a representative linear model for synthesizing a flight controller. Another system identification method that is also suitable for unmanned flying vehicles is referred to as the modeling for flight simulation and control analysis (MOSCA) method [9].

In this paper, the linear quadratic control method is applied to construct a state feedback controller for the quadcopter. This controller is obtained by minimizing a linear quadratic cost function that is subject to the quadcopter linear dynamics [10]. It is assumed that information about all state variables of the quadcopter is available for feedback control. The aims of applying this controller are to stabilize the quadcopter at the equilibrium point and also to allow the quadcopter to track a reference input [11]. An example based on the quadcopter model for hovering flight [7] is presented to illustrate the performance of the resulting linear quadratic controller.

The rest of this paper is organized as follows. Section 2 presents the equations of motion of the quadcopter underlying the derivation of the linear state-space model used for synthesizing the linear quadratic controller. Section 3 shows an example about applying the optimal linear quadratic control method to synthesize the stabilizing controller for the quadcopter. Finally, concluding remarks are presented in Section 4.

2 Problem Formulation

2.1 Equations of Motion

A quadcopter is commonly considered as an aircraft which can move freely in six degrees of freedom within an air space. Thus, during its flight, the quadcopter is capable of simultaneously performing translational and rotational motions driven by external forces and torques/moments, respectively. To properly utilize the quadcopter for practical applications, it is then necessary to grasp such motions through a mathematical model derived based on physical laws. A suitable mathematical model about the rigid-body dynamics of the quadcopter is usually presented in terms of equations of motions. These equations can be derived based on the Newton's second law of motion and the kinematic principles of a moving reference frame [12, 13]. That is,

$$\begin{aligned}\mathcal{F} &= m\dot{v} + m(\omega \times v) \\ \mathcal{M} &= I\dot{\omega} + (\omega \times I\omega)\end{aligned}\quad (1)$$

Each physical quantity vector of the quadcopter dynamics equations (1) has three components in the \mathbb{R}^3 space (except m) and is described as follows:

\mathcal{F}, \mathcal{M} : external forces and torques/moments acting on the quadcopter,

m, I : mass and moment of inertia,

v, ω : translational velocities and angular rates

where $\mathcal{F} = [X \ Y \ Z]^T$, $\mathcal{M} = [L \ M \ N]^T$, $I = [I_{xx} \ I_{yy} \ I_{zz}]^T$, $v = [u \ v \ w]^T$ and $\omega = [p \ q \ r]^T$. Thus, the quadcopter equations of motion are expressed as follows:

$$\mathcal{F} = \begin{bmatrix} X \\ Y \\ Z \end{bmatrix} = m \begin{bmatrix} \dot{u} + qw - rv \\ \dot{v} + ru - pw \\ \dot{w} + pv - qu \end{bmatrix}, \quad (2)$$

$$\mathcal{M} = \begin{bmatrix} L \\ M \\ N \end{bmatrix} = \begin{bmatrix} I_{xx}\dot{p} - (I_{yy} - I_{zz})qr \\ I_{yy}\dot{q} - (I_{zz} - I_{xx})pr \\ I_{zz}\dot{r} - (I_{xx} - I_{yy})pq \end{bmatrix}.$$

The quadcopter is typically powered up by four motors mounted on the tips of its arms. A fixed-pitch propeller is installed on each motor to produce thrust that can be varied to propel and control the quadcopter's motion. Thus, incorporating the gravitational and control forces, the equations of motion in (2) can be enhanced to have the form as follows:

$$\left\{ \begin{array}{l} \dot{u} = rv - qw - g \sin \theta + a_x \\ \dot{v} = pw - ru + g \sin \theta \cos \theta + a_y \\ \dot{w} = qu - pv + g \sin \theta \cos \theta + \frac{\delta_t}{m} \\ \dot{p} = \frac{(I_{yy} - I_{zz})qr + \delta_a}{I_{yy}}, \\ \dot{q} = \frac{(I_{zz} - I_{xx})pr + \delta_e}{I_{yy}} \\ \dot{r} = \frac{(I_{xx} - I_{yy})pq + \delta_r}{I_{zz}} \end{array} \right. \quad (3)$$

2.2 A Linear State-Space Model

The quadcopter's dynamic equations in (3) can concisely be written in the form of a single nonlinear differential equation as follows:

$$\dot{x} = f(x, u) \quad (4)$$

where $x = [u \ v \ w \ p \ q \ r \ \phi \ \theta \ \psi]^T$ is the state vector $u = [\delta_t \ \delta_a \ \delta_e \ \delta_r]^T$ is the control input vector and $f(\cdot)$ is a vector-valued nonlinear function of x and u . Each component of x and u are described as follows [7]:

- u, v, w : longitudinal, lateral and vertical velocities,
- p, q, r : roll, pitch and yaw rates,
- ϕ, θ, ψ : roll, pitch and yaw angles,
- δ_t : heave control input,
- δ_a : roll control input,

δ_e : pitch control input,

δ_r : yaw control input.

For the purpose of linear controller design, it is reasonable to linearize the nonlinear dynamic equation (4) about an equilibrium point (x_{eq}, u_{eq}) via the Taylor series expansion. At the equilibrium point (x_{eq}, u_{eq}) the quadcopter is said to be in a trim condition, where all forces and moments acting upon the quadcopter are balance. Consequently, the nonlinear dynamic equation (4) is equal to zero, that is $(x_{eq}, u_{eq}) = 0$.

The state trajectory and control input of the quadcopter about the equilibrium point (x_{eq}, u_{eq}) are given by

$$x = x_{eq} + \Delta x, \quad u = u_{eq} + \Delta u. \tag{5}$$

Thus, by taking only the first-order terms of the Taylor series expansion of the nonlinear dynamic equation (4), one may obtain a linear state-space model as follows:

$$\Delta \dot{x} = A \Delta x + B \Delta u, \tag{6}$$

where $A = \partial f / \partial x$ and $B = \partial f / \partial u$ are Jacobian matrices evaluated at the equilibrium point (x_{eq}, u_{eq}) . For simplicity, the symbol Δ in (6) will be removed subsequently.

Referring to (3), one may obtain the A and B matrices in (6) as follows [7, 8]:

$$A = \begin{bmatrix} X_u & 0 & 0 & 0 & X_q & 0 & 0 & -g & 0 \\ 0 & Y_v & 0 & Y_p & 0 & 0 & g & 0 & 0 \\ 0 & 0 & Z_w & 0 & 0 & 0 & 0 & 0 & 0 \\ 0 & L_v & 0 & L_p & 0 & 0 & 0 & 0 & 0 \\ M_u & 0 & 0 & 0 & M_q & 0 & 0 & 0 & 0 \\ 0 & 0 & 0 & 0 & 0 & N_r & 0 & 0 & 0 \\ 0 & 0 & 0 & 1 & 0 & 0 & 0 & 0 & 0 \\ 0 & 0 & 0 & 0 & 1 & 0 & 0 & 0 & 0 \\ 0 & 0 & 0 & 0 & 0 & 1 & 0 & 0 & 0 \end{bmatrix}, \quad B = \begin{bmatrix} 0 & 0 & X_{\delta_e} & 0 \\ 0 & Y_{\delta_a} & 0 & 0 \\ Z_{\delta_t} & 0 & 0 & 0 \\ 0 & L_{\delta_a} & 0 & 0 \\ 0 & 0 & M_{\delta_e} & 0 \\ 0 & 0 & 0 & N_{\delta_r} \\ 0 & 0 & 0 & 0 \\ 0 & 0 & 0 & 0 \\ 0 & 0 & 0 & 0 \end{bmatrix} \tag{7}$$

Here, g is the gravitational acceleration and other unknown non-zero entries of the A and B matrices denote the stability derivatives of the forces and moments with respect to the corresponding state variables x_i (for $i = 1, 2, \dots, 9$) and control inputs u_j (for $j = 1, \dots, 4$).

2.3 Optimal Linear Quadratic Control

Stabilization problem. Given the linear time-invariant state-space model (6), (7) of the quadcopter, one may design a state-feedback controller by minimizing a linear-quadratic cost function as follows [10]:

$$J = \int_0^{\infty} [x(t)^T Q x(t) + u(t)^T R u(t)] dt \quad (8)$$

Where $Q \in \mathbb{R}^{n \times n}$, $Q \geq 0$, and $R \in \mathbb{R}^{m \times m}$, $R > 0$ are weighting matrices. The desirable state-feedback controller is of the form

$$u(t) = Kx(t) \quad (9)$$

where $K \in \mathbb{R}^{m \times n}$ is the state-feedback controller gain matrix. Applying the state feedback controller (9) to the open-loop state-space model (6) and (7) of the quadcopter, one obtains a closed-loop system given as follows:

$$\dot{x}(t) = (A + BK)x(t). \quad (10)$$

Thus, the controller gain matrix K is such that the matrix $(A + BK)$ is Hurwitz in order to result in an asymptotically stable closed-loop system. This control problem is commonly known as a stabilization or regulation of an open-loop linear system around its equilibrium point and is solvable if (A, B) is stabilizable. The resulting closed-loop system is then enabled to return to the equilibrium point by eliminating the effect of any non-zero initial conditions. Such a controller is then called a linear quadratic regulator [12, 13].

To obtain such a stabilizing controller that minimizes the cost function (8), one is then required to find a symmetric matrix $P > 0$, $P \in \mathbb{R}^{n \times n}$ as a solution to an algebraic Riccati equation:

$$A^T P + PA + Q - PBR^{-1}B^T P = 0 \quad (11)$$

Therefore, the controller gain matrix K can be constructed as

$$K = -R^{-1}B^T P \quad (12)$$

and the minimal cost function value J^* is given as

$$J^* = x(0)^T P x(0). \quad (13)$$

When synthesizing a desirable controller to satisfy stability and performance criteria of a closed-loop system, one has to appropriately determine the weighting matrices Q and R . To serve this purpose, it is quite common to choose Q and R as diagonal matrices. Thus, they can be interpreted as penalties corresponding to each state and control input variables, respectively. Although the weighting matrices Q and R are in general not unique, one may follow the Bryson's rule to set their diagonal entries [10]. That is,

$$q_{ii} = \frac{1}{\text{maximum admissible value of } x_i^2}, \quad i = 1, 2, \dots, n, \quad (14)$$

$$r_{jj} = \frac{1}{\text{maximum admissible value of } u_j^2}, \quad j = 1, 2, \dots, m.$$

Tracking problem. In practice, one may not only be interested in stabilizing the open loop system, but also in tracking a reference input. To achieve this control objective, one needs to first define an output variable $y \in \mathbb{R}^p$ required to follow the reference input $r \in \mathbb{R}^p$. That is,

$$y(t) = Cx(t), \quad (15)$$

where $C \in \mathbb{R}^{p \times n}$ is the output matrix. Thus, to design a state-feedback controller of the form (9) such that the output y will track the reference input r , one may follow the same procedure to design the controller gain matrix K as above. In other words, the tracking control problem can be solved by transforming it into the stabilization problem.

In this regard, an error variable variable $e \in \mathbb{R}^p$ is defined such that

$$\begin{aligned} e(t) &:= er(t) - y(t), \\ \dot{e}(t) &:= \dot{e}(t). \end{aligned} \quad (16)$$

Now, combining (6), (15) and (16), one may obtain an augmented open-loop system:

$$\begin{aligned} \dot{\bar{x}}(t) &= \bar{A} \bar{x}(t) + \bar{B}u(t) + B_r r(t), \\ y(t) &= \bar{C} \bar{x}(t), \end{aligned} \quad (17)$$

where

$$\bar{x}(t) = \begin{bmatrix} z(t) \\ x(t) \end{bmatrix}, \quad \bar{A} = \begin{bmatrix} 0 & C \\ 0 & A \end{bmatrix}, \quad \bar{B} = \begin{bmatrix} 0 \\ B \end{bmatrix}, \quad B_r = \begin{bmatrix} I \\ 0 \end{bmatrix}, \quad \bar{C} = [0 \quad C]. \quad (18)$$

Note that 0 and I are zero and identity matrices with appropriate dimensions, respectively. To track the reference input r , it is thus necessary to stabilize the

augmented open-loop system (18) by applying the state-feedback controller of the form (9). That is,

$$u(t) = \bar{K}\bar{x}(t), \quad \bar{K} = [K_z \quad K_x] \quad (19)$$

where $K_z \in \mathbb{R}^{m \times p}$ and $K_x \in \mathbb{R}^{m \times n}$. The resulting closed-loop system can then be written as

$$\dot{\bar{x}}(t) = A_c \bar{x}(t) + B_r r(t) \quad (20)$$

where

$$A_c = \begin{bmatrix} 0 & -C \\ BK_e & A + BK_x \end{bmatrix} \quad (21)$$

is Hurwitz.

Since the closed-loop system (20) is asymptotically stable, $\dot{z}(t)$ and $\dot{x}(t)$ will converge to zero as time t goes to infinity. This implies that $y(t)$ will be equal to $r(t)$ at the steady state. In this way, the tracking control problem has been solved by incorporating an integral control action into the closed-loop system (20). In fact, this approach will also render the closed-loop system (20) robust against perturbations due to bounded exogenous disturbances.

3 Controller Synthesis

In this section, a state-feedback controller is designed for the quadcopter based on a linear dynamic model for hovering flight. Thus, the parameter values in the linear statespace model (6) and (7) are given as follows [7]:

$$\begin{array}{lll} X_u = -0.0429, & Y_p = 0.0000, & Y_{\delta_a} = -0.2016, \\ Y_v = -0.0429, & L_p = 0.0000, & Z_{\delta_t} = -0.7414, \\ Z_w = 0.0000, & M_q = 0.0000, & L_{\delta_a} = 0.7066, \\ L_v = -0.4376, & N_r = -0.5231, & M_{\delta_e} = 0.6662, \\ M_u = 0.5241, & X_{\delta_e} = 0.2269, & N_{\delta_r} = 0.1306, \\ X_q = 0.0000, & & \end{array} \quad (22)$$

and the gravitational acceleration g is 32.17 ft/s^2 .

Let us consider the case where the quadcopter is required to track lateral (roll), longitudinal (pitch) and directional (yaw) reference inputs. The state-feedback controller can be obtained by applying the linear quadratic control method described in sub-

Section 2.3. For this example, the weighting matrices $Q := \text{diag}[q_\bullet]$ and $R := \text{diag}[r_\bullet]$ are chosen to be diagonal matrices with the following entries:

$$\begin{aligned}
 q_{z_\phi} &= 1 \times 10^4, & q_{z_\theta} &= 1 \times 10^4, & q_{z_\psi} &= 1 \times 10^4, \\
 q_u &= 0.5, & q_v &= 0.5, & q_w &= 0.5, \\
 q_p &= 5.0, & q_q &= 5.0, & q_r &= 5.0, \\
 q_\phi &= 1 \times 10^2, & q_{\theta'} &= 70.0, & q_\psi &= 5 \times 10^3. \\
 r_{\delta_t} &= 4.0, & r_{\delta_a} &= 0.5, & & \\
 r_{\delta_e} &= 1.0, & r_{\delta_r} &= 2.0, & &
 \end{aligned} \tag{23}$$

Here, the subscripts \bullet of q_\bullet and r_\bullet denote the state and control input variables of the augmented open-loop system (17).

The controller gain matrix \bar{K} can then be computed using the command `lqr` of MATLAB. Moreover, the efficacy of the resulting controller can be demonstrated using Simulink. Examples of tracking reference inputs for roll, pitch and yaw angles are considered, respectively. The time responses of these angular quantities are shown in Figures 1, 2, and 3. It is obvious that the resulting controller is indeed able to stabilize the closed-loop system and also to allow the respective state variables to track the given reference inputs with zero steady-state errors.

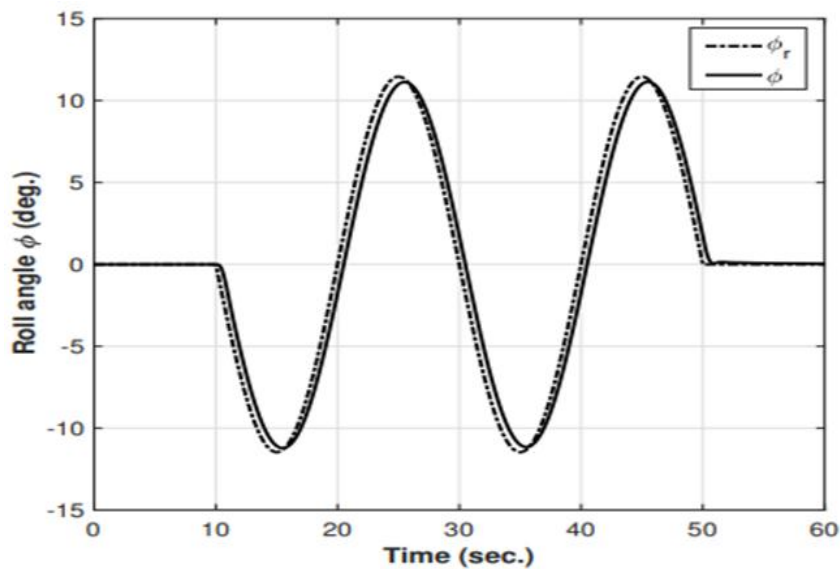


Figure 1. The time response of the roll angle ϕ due to the sinusoidal reference input ϕ_r

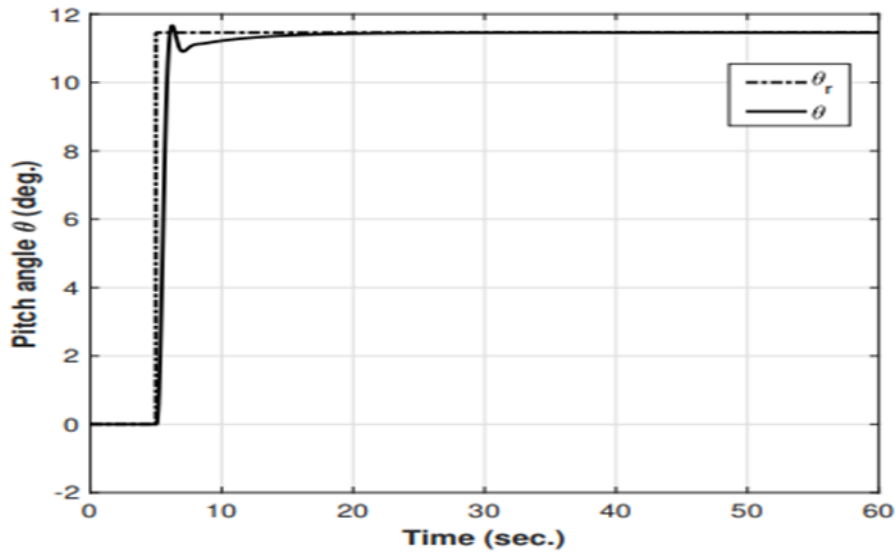


Figure 2. The time response of the pitch angle θ due to the step reference input θ_r .

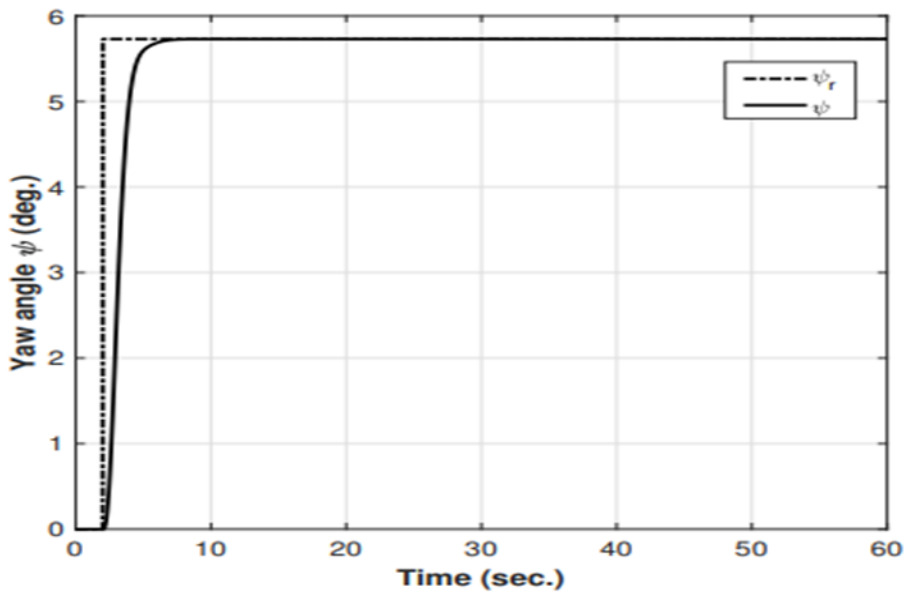


Figure 3. The time response of the yaw angle ψ due to the step reference input ψ_r .

4 Conclusions

This paper has presented the optimal linear quadratic control method to synthesize a state-feedback controller for the quadcopter. The resulting controller is effective not only to stabilize the quadcopter, but also to enable some state variables to track the given reference inputs. The tracking capability is facilitated by the integral control action incorporated into the closed-loop system. If the reference input is considered as a

perturbing exogenous input, it is then clear that the closed-loop system is robust against such a perturbation. The current results can be extended to consider other control methods to address an output-feedback control problem with uncertainty related to the quadcopter model. Furthermore, a more complex control problem can also be considered where there are multiple quadcopters flying in formation within a network.

Acknowledgements

This work was supported by the Laboratory of Distributed Aerospace Systems and Control within the Department of Aerospace and Software Engineering, Gyeongsang National University, Jinju, Republic of Korea. The author also would like to thank Dr. Sudi Mungkasi for the opportunity to publish this paper in the International Journal of Applied Sciences and Smart Technologies.

References

- [1] G. Cai, J. Dias, and L. Seneviratne, "A survey of small-scale unmanned aerial vehicles: Recent advances and future development trends," *Unmanned Systems*, **2** (2), 175–199, 2014.
- [2] M. Hassanalian and A. Abdelkefi, "Classifications, applications, and design challenges of drones: A review," *Progress in Aerospace Sciences*, **91**, 99–131, 2017.
- [3] G. Hoffmann, H. Huang, S. Waslander, and C. Tomlin, "Quadrotor helicopter flight dynamics and control: Theory and experiment," in *Proceedings of the AIAA Guidance, Navigation and Control Conference and Exhibit*, 1–20, August 2007.
- [4] F. Rinaldi, S. Chiesa, and F. Quagliotti, "Linear quadratic control for quadrotors uavs dynamics and formation flight," *Journal of Intelligent & Robotic Systems*, **70** (1–4), 203–220, 2013.
- [5] J. -J. Xiong and E. -H. Zheng, "Position and attitude tracking control for a quadrotor UAV," *ISA Transactions*, **53** (3), 725–731, 2014.
- [6] H. Mo and G. Farid, "Nonlinear and adaptive intelligent control techniques forquadrotoruav—a survey," *Asian Journal of Control*, **21** (2), 989–1008, 2019.

- [7] W. Wei, M. B. Tischler, and K. Cohen, “System identification and controller optimization of a quadrotor unmanned aerial vehicle in hover,” *Journal of the American Helicopter Society*, **62** (4), 1–9, 2017.
- [8] M. B. Tischler and R. K. Remple, *Aircraft and Rotorcraft System Identification*, American Institute of Aeronautics and Astronautics, Virginia, 2012.
- [9] M. L. Civita, W. C. Messner, and T. Kanade, “Modeling of small-scale helicopters with integrated first-principles and system-identification techniques,” *Proceedings of the 58th Forum of the American Helicopter Society*, pp. 2505–2516, June 2002.
- [10] J. P. Hespanha, *Linear Systems Theory*, Princeton University Press, New Jersey, 2nd edition, 2018.
- [11] M. Kanamori and M. Tomizuka, “Dynamic anti-integrator-windup controller design for linear systems with actuator saturation,” *Journal of Dynamic Systems, Measurement and Control*, **129** (1), 1–12, 2007.
- [12] B. Mettler, *Identification Modeling and Characteristics of Miniature Rotorcraft*, Springer, New York, 2003.
- [13] G. D. Padfield, *Helicopter Flight Dynamics*, Blackwell Publishing, Oxford, 2nd edition, 2007.

Development of Stamping Machine Module to Improve Practical Competency

Pippie Arbiyanti

*Department of Mechatronics, Politeknik Mekatronika Sanata Dharma,
Yogyakarta, Indonesia*

Corresponding Author: pipie@pmsd.ac.id

(Received 20-05-2019; Revised 17-10-2019; Accepted 17-10-2019)

Abstract

The aim of this research is to design and manufacture a stamping machine module controlled by PLC. Stamping machine is an application of electro-pneumatic system in industry to print image/text on the workpieces. The result of this research is a stamping module controlled by PLC, with reliable and easy to disassemble for learning Electro-pneumatic Practice.

Keywords: stamping, electro-pneumatic system, automation, PLC

1 Introduction

Entering the era of industrial revolution 4.0, more industries are implementing automation in their production processes. Thus, the need for workers who have expertise in accordance with the latest technological developments is increasing. Vocational education in engineering subject as a provider of skilled workers needs to equip students with skills that are in line with the latest technological developments.

One of the important components in industrial automation is the electro-pneumatic system. This electro-pneumatic system is widely used in the production process because it uses a cheap, clean and effective source of wind power. Knowledge and skills about electro-pneumatic is a mandatory skill that must be possessed by a technician in the industry. The competencies needed from this electro-pneumatic system are

understanding of electrical and pneumatic components, functions, working principles, and how to control them; as well as assembling skills, troubleshooting, and commissioning of an electro-pneumatic system.

In the field of education, the delivery of electro-pneumatic material is provided using practical teaching aids. The disadvantage of this props is that the types of components provided are limited, so that what can be done is the demonstration/simulation of the motion of an electro-pneumatic system. Thus students have not yet gotten a real picture of an electro-pneumatic system as in the industry. Then we need examples of production processes that are close to reality with the industrial world, one of which is the stamping process [1]. The process of stamping, is the process of printing images / text on workpieces automatically. Some manufacturers such as Festo and SMC have offered practice modules that are examples of automation processes in the industry, but at very high prices [2, 3]. Singh [4] has also developed automatic press machines using pneumatic for large scale.

This paper offers the design and manufacturing of stamping machine modules with PLC control. This module will be used as an electro-pneumatic practice prop. This module can be disassembled with the appropriate equipment, to meet the competencies of students in assembling skills, troubleshooting, and programming in an electro-pneumatic system. In addition, the cost of making modules in this paper is much cheaper than existing modules because they are self-developed and use used components that can still function properly.

The paper is organized as follows: Section 2 presents the module design while the method (steps) of making the module will be described in Section 3. The results of the research and discussion are written in Section 4. This paper concludes with some conclusions.

2 Design

In this section, the writer explains the design of the proposed tool, which is stamping process and mechanical design.

2.1. Stamping Process Design

Stamping machine module used to stamp double-sided workpieces using tampon stamping method. This machine involves a sequence of operations illustrated in Figure 1 below.

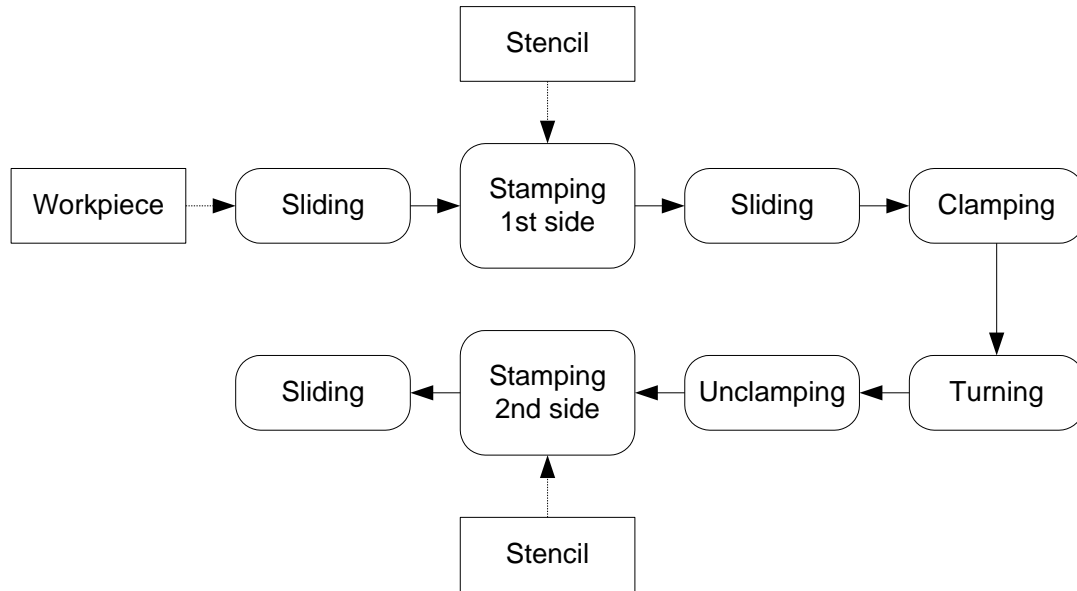


Figure 1. Stamping process

Stamping process starts by putting the workpiece on the conveyor belt, which will carry the workpiece to the stamping station. A plunger tampon will stamp the workpiece. The workpiece, which has already been stamped on one side, moves between the gripper jaws, and then closes. The workpiece is lifted, reversed, then lowered again to the conveyor. The stamping process will be repeated at the second station to stamp another side. After the two sides are printed, the workpiece will run towards the storage box.

2.2. Mechanical Design

This stamping module is designed to be easily disassembled, to meet desired practice competencies. Mechanical module design is presented in Figure 2.

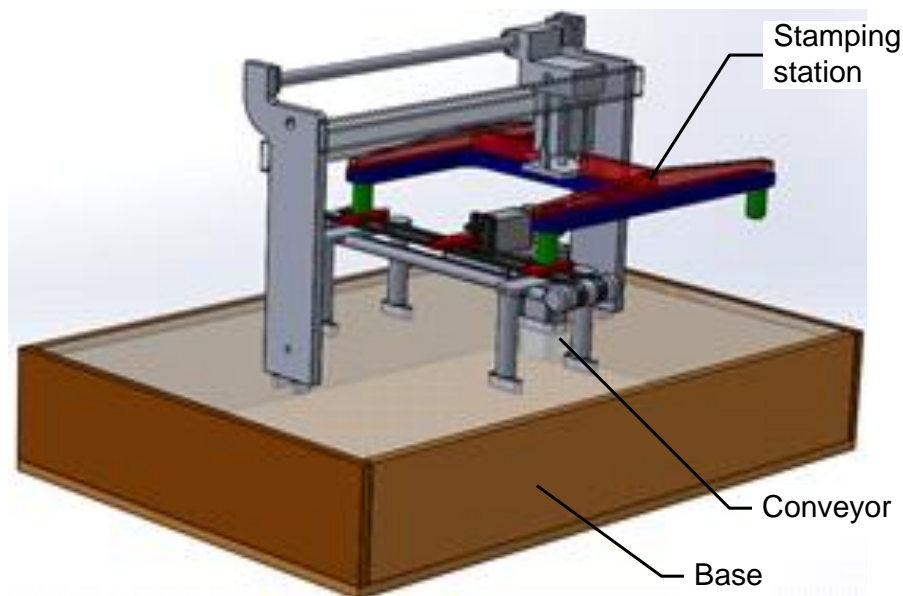


Figure 2. Mechanical design of stamping machine

The base is to put the control components, namely power supply, solenoid valve, and PLC. The upper part is to put a stamping machine that consists of a conveyor with timing belt and a pneumatic system to meet the stamping process. The module should be able to be dismantled and assembled with the appropriate tools.

3 Research Methodology

This section is devoted for the research method. Stamping machine module is done by pneumatic system with PLC-based controller.

3.1. Pneumatic System

The actuator used to carry out the stamping process is:

- a) Sliding is done by a DC motor, which is actuating belt-conveyor.
- b) Two tampon plungers actuated by a rodless cylinder.
- c) A Parallel gripper is used to clamping the workpiece.
- d) A semi-rotary drive is used to hold the gripper.
- e) Two lifting cylinder used to move-up and down the semi-rotary unit and tampon plunger.

The pneumatic stamping machine circuit is shown in Figure 3 below. Drawing and simulation pneumatic circuit are carried out using the Fluid SIM-P software [5].

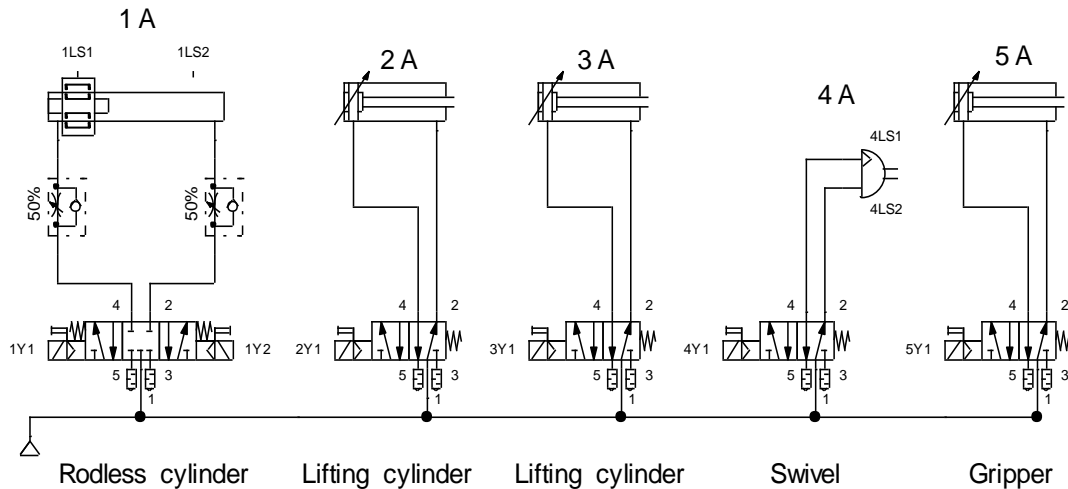


Figure 3. Pneumatic circuit

3.2. PLC-based Controller

This stamping machine is controlled by PLC OMRON. The various inputs and outputs are shown in Table 1.

Table 1. PLC inputs/outputs

Digital inputs	Digital outputs
Start	Motor M1
Stop	Solenoid 1Y1
Reset	Solenoid 1Y2
Manual/Auto M/A	Solenoid 2Y1
Emergency stop	Solenoid 3Y1
Limit switch 1LS1	Solenoid 4Y1
Limit switch 1LS2	Solenoid 5Y1
Limit switch 4LS1	M/A indicator
Limit switch 4LS2	

Limit switches 1LS1 and 1LS2 were placed to know the position of rodless cylinder, which is holding the tampon plunger. Limit switches 4LS1 and 4LS2 were placed to know the position of semi-rotary drive/swivel. Control action was taken according to

the various inputs from the switches. The system can run at manual or automate mode by selecting M/A switch.

The sequential diagram of the PLC program is shown in Figure 4. A ladder logic program for this PLC was written in CX-programmer [6].

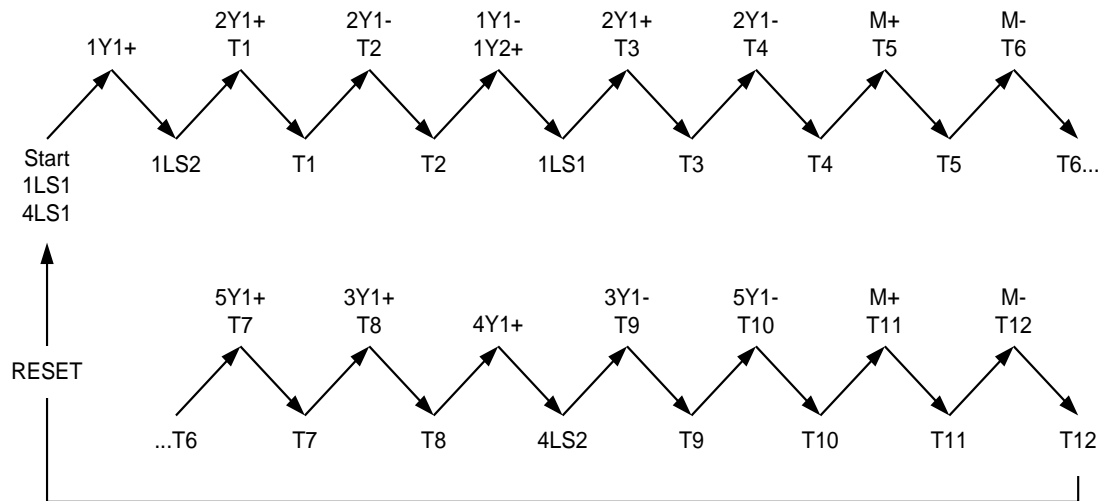


Figure 4. Sequential diagram

4 Results and Discussions.

The results of this research is a stamping machine module as presented in Figure 5 below.



Figure 5. Stamping machine module

Testing the first stage of the stamping machine module is done by running the system in the order of the planned process. The test results show that the module can work well according to the plan.

In Figure 6, the second stage of testing is carried out by students by using it in lectures on Electro-pneumatic Practice at the Mechatronics Department, Politeknik Mekatronika Sanata Dharma (PMSD). In this practice, students conduct assembling, troubleshooting, and programming stamping machine module based on the procedures in the Manual Book. The test results show that students can perform procedures based on the Manual Book to be able to run the stamping machine process properly.



Figure 6. Electro-pneumatic workshop using stamping machine module

5 Conclusions

A PLC-based controller for stamping machine module has been successfully designed and developed. It has been evaluated by simulating the stamping operation on Fluid SIM-P and real running on Electro-pneumatic Workshop.

This module is equipped with a Manual Book that can be used for assembling learning, troubleshooting, and programming a PLC-based electro-pneumatic system. Future studies will focus on developing other automation process modules.

Acknowledgements

This research was financially supported by Polytechnic Education Development Project, Ditjen-DIKTI. The author thanks the colleges of Politeknik Mekatronika Sanata Dharma for some discussions.

References

- [1] S. Hesse, *99 Examples of Pneumatic Applications*, Esslingen: Festo AG & Co, 2001.
- [2] Festo, *Modular System for Mechatronics Training*, Festo Corporation, 2007.
- [3] SMC, “FMS-200:Flexible integrated assembly systems,” SMC International Training, 2019.
- [4] R. Singh and H. K Verma, “Development of PLC-based controller for pneumatic pressing machine in engine-bearing manufacturing plant,” *Procedia Computer Science*, **125** (2), 449–458, 2018.
- [5] Festo, “Fluid SIMR4 Pneumatics User Guide,” March 2006.
- [6] OMRON, “CX-Programmer Ver.9.0,” December 2009.

Saving the Moving Position on the Continuous Passive Motion Machine for Rehabilitation of Shoulder Joints

Antonius Hendro Noviyanto

Politeknik Mekatronika Sanata Dharma, Yogyakarta, Indonesia

Corresponding Author: hendro@pmsd.ac.id

(Received 03-06-2019; Revised 29-10-2019; Accepted 29-10-2019)

Abstract

This paper presents the results of the motion therapy device Continuous Passive Motion (CPM) Machine which is applied to the shoulder joint with storage movement. The process of joint rehabilitation is carried out by continuous passive movements. This movement is intended not to overload the work of the muscles and there is no stiffness in the joints after surgery or stroke patients or patients who have carried out immobilization for quite a long time. The CPM Machine developed can move flexion and horizontal abduction. The position storage in this tool is carried out in a range of movements in flexion and horizontal abduction. With the storage of movement can be done movement/therapy exercises in patients with joint stiffness can be done passively and continuously.

Keywords: CPM machine, joint rehabilitation, flexion, horizontal abduction

1 Introduction

Post-joint surgery patients or patients who are injured in the joints are required to do joint movement exercises. Joint movement exercises can be performed using therapy equipment Continuous Passive Motion Machine (CPM machine) [1]. Basically the

working principle of this tool is to move passively and continuously as needed, so that the joints in patients do not experience stiffness [2].

Joint stiffness can be caused by prolonged immobilization of the shoulder joint due to post joint surgery. In addition, joint stiffness can also be caused by patients who are reluctant to move the joint due to the pain felt by the patient. Based on the results of the interview with Dr. Hermawan Nagar Rasyid, Dr., SpOT., M.T., Ph.D., FICS., therapy for joints of the shoulder can be done with flexion and extension as well as horizontal motion adduction and horizontal abduction.

Joint stiffness can be prevented by providing movement exercises that can restore ROM from the shoulder joint [3]. The movement can be given to patients with passive and repeated joint stiffness. Passive movement is a movement that does not require muscle work. Movement exercises are carried out 3-5 times a day, where each exercise is carried out for 1 hour. Movements that can be given include [4]:

1. Flexion / extension: to reduce tissue adhesions
2. Adduction / abduction: to increase the range of motion of the shoulder
3. Rotational motion: to increase the range of motion of the shoulder

Giving training is done by giving the angle of movement gradually with the recommended speed is 1 rotation in 45 seconds [4]. Long immobilization can lead to joint stiffness. Joint stiffness can be reduced by moving the joints. In patients after joint surgery it is recommended to immediately carry out joint movement exercises, so as to reduce the risk of joint stiffness.

CPM machine is a tool that has a method of rehabilitation of damaged joints [5]. Movement exercises using CPM machines can stimulate healing and regeneration of joint cartilage and prevent joint stiffness. The use of CPM machines has the following benefits [5]:

1. Improve nutrition and metabolic activity on the surface of cartilage.
2. Stimulates mesenchymal cells to differentiate inside the surface of the cartilage.
3. Accelerate healing of cartilage and periarticular tissue, such as tendons and ligaments.

The use of CPM machine that is in accordance with the procedure, is expected to restore the scope of motion of the joints for sufferers of joint trauma/patients post joint surgery [6].

Based on the need for therapeutic tools for the shoulder joint, then in this study a storage test of movement on the CPM Machine therapeutic apparatus was made. So that the therapeutic apparatus can be used repeatedly with the same movement mode according to the storage of movements that have been carried out.

2 Design

CPM Machine that will be designed is a system based on a microcontroller. The system in this tool consists of a microcontroller, DC motor controller, and rotary encoder. The overall system block diagram is shown in Figure 1.

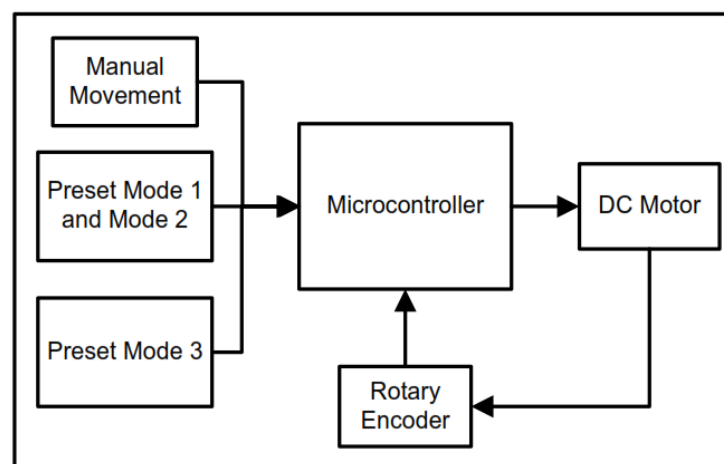


Figure 1. Diagram block system [7]

The therapeutic apparatus that is made can do flexion and horizontal abduction. The flexion movement angle is $20^{\circ} - 120^{\circ}$ and the movement angle from horizontal abduction is $0^{\circ} - 180^{\circ}$. Besides the movement angle, on this tool people can also set the rotational speed of the tool, namely: 1 RPM, 2 RPM, and 3 RPM. The rotating speed in the tool is controlled using PID control [7].

As in Figure 2, the tool has 3 working modes, namely:

1. Mode I : flexion
2. Mode II : horizontal abduction
3. Mode III : save position

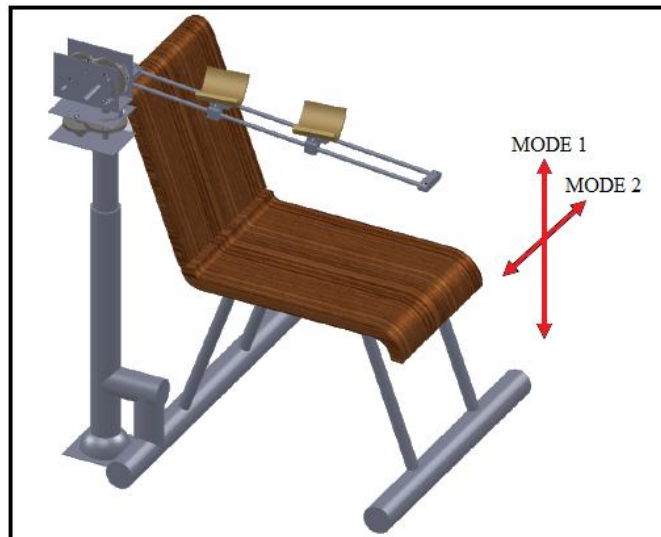


Figure 2. Tool movement mode [7]

In mode I the tool will move flexibly with a movement angle of $20^{\circ} - 120^{\circ}$. In mode II the tool will move horizontally abduction with a movement angle of $0^{\circ} - 80^{\circ}$ [7]. While in mode III the tool moves according to the position that has been saved. The position stored can change according to the needs with a range of flexed and horizontal abduction movements.

The storage system on the device utilizes the memory facilities available on the microcontroller. Data is stored in the form of data on movement angle and desired type of movement (flexion/abduction).

3 Method

The method used in this study is by conducting experiments on tools to get the test results. The results obtained are the results of tool movement angle data and the results of movement based on position storage.

In testing the movement angle of the tool, the method that is carried out is by measuring the movement steps of the tool by using a protractor. The results of these measurements will then be compared with the desired requirements.

Testing the movement in accordance with storage is done by comparing the results of the movement stored in memory from the first cycle to the next cycle.

4 Testing and Discussion

Testing on this tool is done by testing the movement angle and rotational speed of the rotating tool.

4.1 Testing and Discussion of Moving Angles

In flexion movements the measured angles are 30° and 90° , while the horizontal movement of abduction measured angles are 15° and 45° . The results of flexion angle test can be seen in Figure 3.a., while the results of horizontal angle of abduction test can be seen in Figure 3.b.

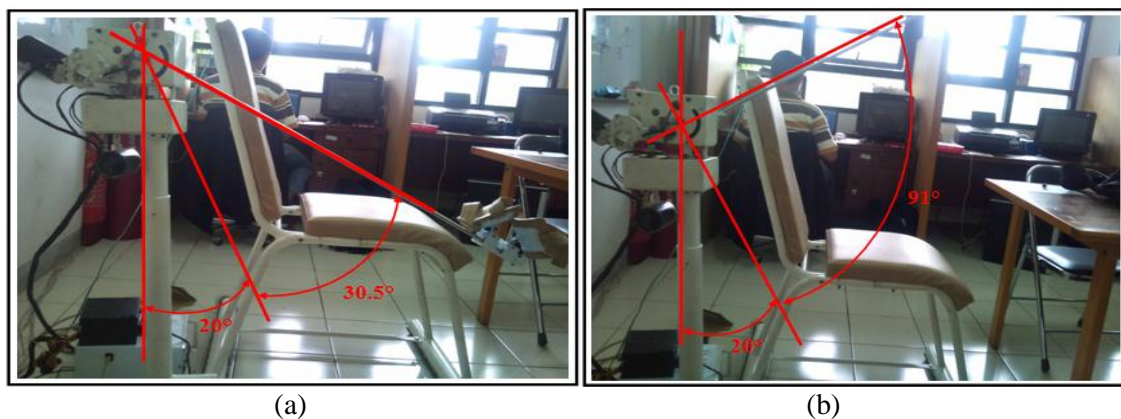


Figure 3. Testing of flexional motion angle: (a) Motion with angle 30° (b) Motion with angle 90°

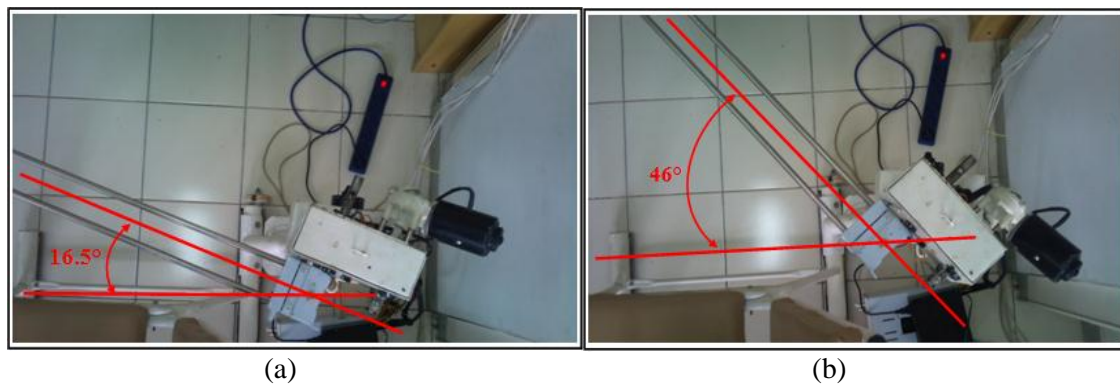


Figure 4. Testing of horizontal motion angles: (a) Motion with angles 15° (b) Motion with angles 45°

The graph in Figure 4 shows the results of motor movement that approaches a straight line. The angle of movement and speed of the tool has a result that is not much different from the settings in the tool. The table of comparison of the results of the movement of the tools and settings in the tool can be seen in Table 1.

Table 1. Moving angle test results

No.	Tool Movement	Desired Angle	Angle Measurement
1	Flexion	30°	30.5°
2		90°	91°
3	Horizontal Abduction	15°	16.5°
4		45°	46°

4.2 Movement Testing and Discussion in Accordance with Position Storage

The arm support that is stored in this position is flexion, abduction, and flexion. Graphs of movement results with position storage can be seen in Figure 5.

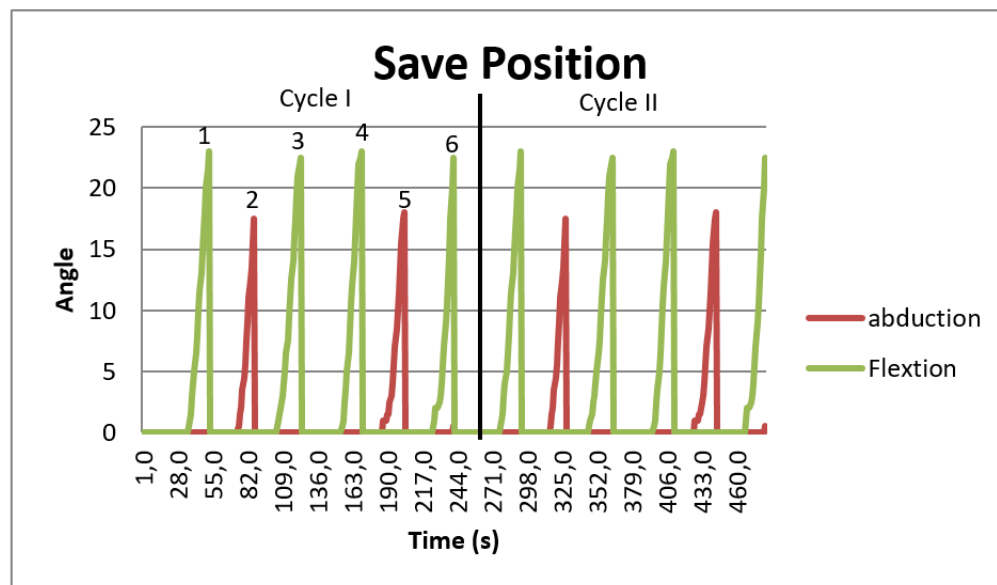


Figure 5. Motion chart with position storage

The position stored in the movement is the movement with the trajectory of flexion and abduction.

Numbers 1, 2, and 3 in the graph show the movement of the arm support. In accordance with the storage of movements that have been carried out, number 1 is a graph of flexion movements. Number 2 in the figure shows a graph of horizontal abduction. While number 3 in the picture shows a graph of flexion movements. The next three movements are movements to return to the starting position. Number 4 is a graph of flexion movements. Number 5 in the figure shows horizontal abduction, where as number 6 from the figure shows flexion. In accordance with the resulting graph, the movement with position storage requires 6 movements for one cycle.

Based on the graph shown, there are similarities in the resulting movement. Movements 1-6 of the first cycle have similarities in movement with movements 1-6 of the second cycle.

5 Conclusion

Based on the results of testing that has been done, the tool can work as needed. Data storage can be carried out and can be implemented on the device. Based on the data

from the movement of the storage, the tool can store movement in accordance with what is needed and can work according to the movements that have been stored.

Acknowledgements

The author thank Dr. Hermawan Nagar Rasyid, SpOT., M.T., Ph.D., FICS who provided information about the need for CPM machine therapy devices.

References

- [1] S. Miyaguchi, N. Matsunaga, K. Nojiri, and S. Kawaji, “Impedance control of CPM device with flex-/extension and pro-/supination of upper limbs,” *IEEE/ASME International Conference on Advanced Intelligent Mechatronics*, 2007.
- [2] S. Miyaguchi, N. Matsunaga, K. Nojiri, and S. Kawaji, “On effective movement in CPM for shoulder joint,” *IEEE International Conference on Systems, Man and Cybernetics*, 2008.
- [3] J. Hamill and K. M. Knutzen, *Biomechanical Basis of Human Movement*, 3rd Edition, Lippincott Williams & Wilkins, USA, 2009.
- [4] Mujianto, *Cara Cepat Mengatasi 10 Besar Kasus Muskuloskeletal dalam Praktik Klinik Fisioterapi*, CV. Trans Info Media, 2013.
- [5] R. B. Salter, *Continuous Passive Motion (CPM): Textbook of Disorders and Injuries of the Musculoskeletal System*, Lippincott Williams & Wilkins, USA, 1999.
- [6] S. W. O'Driscoll and N. J Giori, “Continuous Passive Motion (CPM): theory and principles of clinical application,” *Journal of Rehabilitation Research and Development*, **37** (2), 179–188, 2000.
- [7] A. H. Noviyanto and M. Richard, “Development of therapy equipment for continuous passive motion machine shoulder joints: track motion control,” *ISIET Innovation and Technology in Education for 21st Century Supporting Thailand 4.0*, 2017.

Microcontroller Based Simple Water Flow Rate Control System to Increase the Efficiency of Solar Energy Water Distillation

Elang Parikesit^{1,*}, Wibowo Kusbandono², FA. Rusdi Sambada²

¹ *Politeknik Mekatronika Sanata Dharma, Yogyakarta, Indonesia*

² *Department of Mechanical Engineering, Faculty of Science and Technology, Sanata Dharma University, Yogyakarta, Indonesia*

**Corresponding Author: elang@pmsd.ac.id*

(Received 03-05-2019; Revised 08-06-2019; Accepted 08-06-2019)

Abstract

The current problem of solar energy water distillation is in its low efficiency. Low efficiency is caused by inefficient water evaporation processes. Increasing the efficiency of water evaporation is done by controlling the rate of water entering into the absorber. The commonly used mechanical control system still has weaknesses such as the instability of the water entering the absorber. This causes less effective evaporation of water so that the resulting distillation efficiency is not optimal. The water rate input system for distillation in this study is based on a simple microcontroller. The microcontroller-based input water rate control system allows the rate of input water with a small but continuous flow rate so that the water evaporation process can be more effective. This study aims to improve the efficiency of solar energy water distillation by increasing the efficiency of the water evaporation process through controlling the flow rate of water inlet. The research was carried out by the experimental method. The parameters varied were: the rate of input water which was 0.3 l/hour,

0.5 l/hour and 1.2 l/hour. Parameters measured in this study were: (1) temperature of absorber, (2) temperature of the cover glass, (3) temperature of cooling water, (4) input water temperature, (5) ambient air temperature, (6) distilled water results, (7) solar energy coming in and (8) time of recording data. The results showed that the production of distillation water using microcontroller-based water rate control was a maximum of 523% compared to the model without water rate control at a water flow rate of 0.3 liters / hour, with distillation efficiency of 66%. From the results of this study it can also be concluded that microcontroller based water flow rate controller is more stable than mechanical water flow controller, especially in small flow.

Keywords: microcontroller, rate of input water, distillation of water, solar energy

1 Introduction

Clean water is one of the basic needs of every living thing, but there are still many regions that do not have enough clean water supply, even though the water supply is abundant. The river area is one example that the area has abundant water supply, but there is still a small supply of clean water. The water supply in the area has been contaminated with a lot of dissolved harmful substances. Therefore, a water purification process is needed in one of the processes using distillation. In the distillation process, there are two main processes, namely evaporation and condensation. Factors that can improve the evaporation process include expanding the surface of the liquid, flowing air over the surface, reducing pressure and by heating liquid. While condensation factors, namely temperature, pressure and humidity. The water distillation process starts from evaporation of contaminated water and then condenses on the cover glass. Evaporation does not carry contaminated substances, so the condensed water is suitable for consumption.

The problems that exist in the distillation of solar energy water are the low performance. This is due to the lack of effective evaporation and condensation

processes. The type of distillation that is widely used is the type of tube absorber and the type of fabric absorber. The type of absorber tub is the simplest type of distillation, but the performance produced by this type is among the lowest. The low performance of distillation type absorber tub due to the amount of mass of water that is quite a lot in the tub resulting in the evaporation process does not take place quickly. The type of fabric absorber has better performance than the type of tub absorber. This is due to the type of fabric absorber, the water that will be distilled is flowed to the fabric so that it will produce a thin layer of water on the fabric and cause the water to evaporate faster.

The important thing to get a thin layer on the fabric is to regulate the flow rate of water entering the absorber. Setting the flow rate must be able to produce a constant flow at a small flow rate. Setting the flow of absorber water in cloth distillation is generally carried out mechanically for example using a tap. Mechanical flow rate regulation using a tap cannot produce a constant flow especially at a small flow rate. This study will overcome these problems by using flow settings based on microcontroller.

2 Literature Review

The performance of a solar energy distillation device is determined by the amount of clean water that can be produced, based on the variations used [1]. Many factors that influence the amount of distilled water produced include: the effectiveness of absorber in absorbing solar energy [2], the effectiveness of glass in condensing water vapor [3], the amount of mass / volume of water contained in distillation devices, the surface area of water to be distilled length of heating time, and temperature of water entering the distillation device [4]. Absorber must be made of material with good absorptivity of solar energy, to increase absorptivity generally the absorber is painted in black. The cover glass should not be too hot because if the glass is too hot the steam will be difficult to condense. The amount of mass / volume of water in a distillation device should not be too much because it will prolong the heating process. The flow rate that is too large will cause the evaporation process to be ineffective, but if it is too small then the distillation tool will be easily damaged due to overheating. Therefore, it is necessary

to regulate a good mass flow rate. The setting of the mass flow rate commonly used is a mechanical controller using a tap. Mechanical water flow control has a disadvantage, namely the unstable water flow rate. This is due to the flow with the mechanical arrangement easily blocked by the presence of water vapor that appears on the valve tap. Basically this research aims to overcome the weaknesses in the mechanical water rate control system using a microcontroller based flow rate controller.

3 Method

Experiments are carried out indoors using lamp heat energy as a simulation of solar thermal energy. In experimental data retrieval, several variables used for analysis will be measured. These variables are: temperature absorber in the distillation model ($T_w, ^\circ C$), glass temperature ($T_c, ^\circ C$), lamp heat energy ($G_T, W/m^2$), the amount of distilled water produced (md, liter), the area of distillation equipment (A_c, m^2) and cloth discharge (incoming discharge of distillation equipment; Q liter/hour). In detail, the steps of this research experimentally are :

1. Prepare a distillation device namely a type of distillation cloth with insulated cloth (Figure 1).
2. Preparing measuring instruments to be used include temperature sensors, level sensors, solar meters, arduino microcontrollers, and stopwatches.
3. Regulate the discharge of cloth (the discharge into the distillation apparatus) is 0.3 liters/hour.
4. Record temperature absorber in the distillation model (T.w), glass temperature (T.C), amount of distilled water produced (m_{uap}) and heat energy from the infrared lamp (G_T) every minutes for 8 hours.
5. Repeat steps 2, 3, and 4 with variations in the flow rate of 0.5 liters/hour and 1.2 liters/hour.
6. Perform data analysis compared to the results of distillation water and efficiency resulting from variations number 1, 2, and 3.

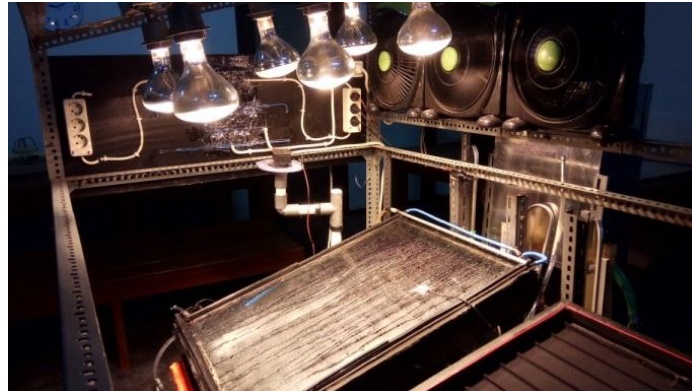


Figure 1. Distillation with fabric and cooler spray

Data collection for each variation was carried out for 3 days and within a day for 8 hours. Data recording is done by sensors arranged with a microcontroller, so data can be collected every minute. Data analysis and discussion of the phenomena that occur is done by making a comparison chart of the increase in water yield per 40 minutes for 8 hours of data collection for each variation. After data collection and data analysis is complete, the research is continued with the compilation of data results and processing, drawing conclusions and suggestions.

The efficiency of solar energy distillation equipment is defined as the ratio between the amount of energy used in the evaporation process of water and the amount of solar radiation that comes during a certain time. The efficiency of a distillation device consists of theoretical and actual efficiency. Theoretical efficiency (η theoretical) is defined as the ratio of the amount of energy used to raise the temperature of a number of water masses in a distillation device based on theoretical data (using solar thermal energy). Where as the actual efficiency (η actual) is defined as the ratio between the amount of energy used to raise the temperature of a number of water masses in a distillation device based on research data collection (using lamp heat energy). The actual efficiency (η actual) can be calculated by Equation 1 and with md is the result of distilled water (liter) is the discharged of cloth, hfg is latent heat of water (J/kg), Ac is the area of distillation (kg), G_T is heat energy lamp (W/m^2).

$$\eta_{aktual} = \frac{md \cdot hfg}{Ac \cdot \int_0^t G_T dt} \quad (1)$$

The efficiency of the η actual distillation tool can be calculated by m_d is the result of distilled water (kg), h_{fg} is the latent heat of evaporation (J/kg), A_c is the distillation area (m^2), GT is the heat energy of the infrared lamp (W/m^2), dt is heating time (seconds).

The control of water flow that will be used in this study is the arrangement of microcontroller and mechanical water flow (as a comparison). Figure 2 shows a block diagram of the water rate control system along with the data acquisition. The system consists of 3 inputs (flow speed setting, water level sensor, and real time clock). While the output is to drive the motor at the peristaltic pump. The function of this system is to control flow rate of water, read the water level that has been achieved, and save the results into memory.

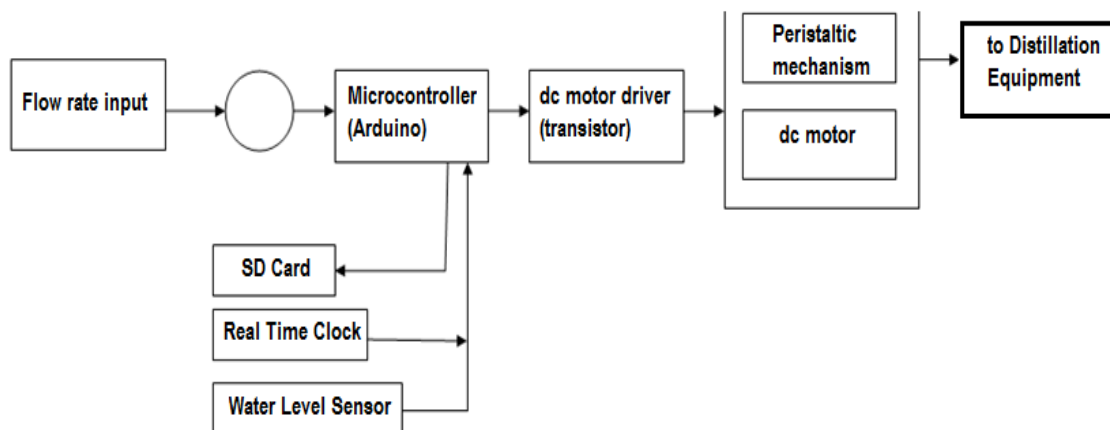


Figure 2. Block diagram of a water flow controller

A peristaltic pump is used in this study to regulate the water input rate (Figure 3) which is controlled by a microcontroller. The microcontroller used is ATmega 328 in the Arduino platform, which consists of hardware and software. The hardware consists of an on-board processor and I/O . While the software consists of the program and boot loader. In this system an Arduino Uno board which has 20 Digital Output and Input pin is used, which consists of pin $D0$ to $D13$ (14 pieces) and added pin $A0 - A5$ (6 pieces). Pin $A0 - A5$ can be used digitally as $D14 - D19$ in the program. Especially for pin $D0$ and $D1$, they are used as communication line to computer [5].



Figure 3. Physical appearance of a peristaltic pump

Peristaltic pumps are positive displacement pumps that are usually used to pump fluids. This pump works by moving a wheel that presses a flexible hose to move fluid [6]. Figure 4 shows the part in the peristaltic mechanism.

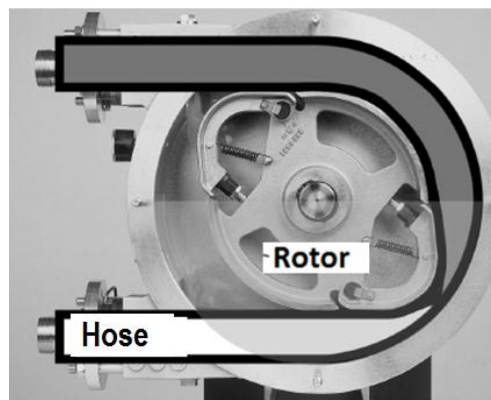


Figure 4. Inner view of peristaltic mechanism

Several studies related to regulating the flow of water with small discharges have been widely carried out. For example to regulate the flow of hospital equipment such as infusion pumps or flow control in the desalination process. Caraballo [7] has conducted research on the use of peristaltic motors with Arduino microcontroller boards to regulate water flow in the desalination process at a low cost. Banerjee et al. [8] also used a microcontroller and peristaltic pump on a dispenser system for mixing 2 types of microfluidic fluid.



Figure 5. Physical appearance of eTape sensor

The water rate control system made in this study is open loop, so the accuracy of the results depends on calibration. The way the water rate control system works is as follows: potentiometer is used to adjust the amount of input voltage to the microcontroller (0-5 volts). Based on the input voltage the microcontroller will regulate the output voltage to the motor. The size of the voltage given to the motor will determine the motor's rotational speed. The Pulse Width Modulation (PWM) signal with a value of 0 – 1023 from Arduino will determine the value of the voltage (0 – 12 volts) given to the motor, the greater the voltage, the faster the motor rotation. The output current of the microcontroller is relatively small (maximum 40 mA). In order to be strong enough to move the motor, the analog output current of the microcontroller must be amplified, in this case using a transistor as an amplifier. The rotation of the DC motor will move the peristaltic mechanism (pulse suppression). For data retrieval (data logging), a memory module (SD Card) is added to the microcontroller. Real Time Clock (RTC) module is also added to provide real time values. While the water level is read by the eTape water level sensor. eTape from Miletone Technologies is a solid state sensor for measuring fluid height [9]. The eTape liquid level sensor is an innovative solid state sensor that does not use mechanical buoys as in general, but uses printed electronics. eTape gets hydrostatic pressure by the fluid where it is immersed, and produces a change in resistance corresponding to the distance from the top of the sensor to the surface of the fluid. The physical form of the eTape sensor is shown in Figure 5.

E-tape can be modeled as a variable resistor ($60 - 550 \Omega \pm 20\%$). In operation, when the liquid level rises the resistance will decrease. If the water level drops resistance will rise. The typical output characteristics of the eTape sensor are shown in Figure 6 below

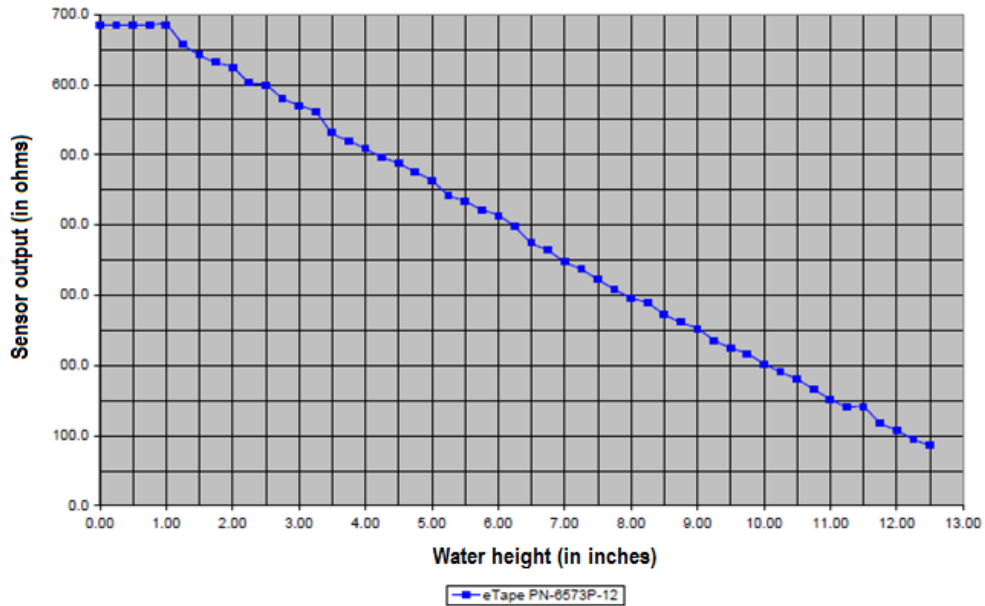


Figure 6. Plot of water height vs resistance of an eTape sensor

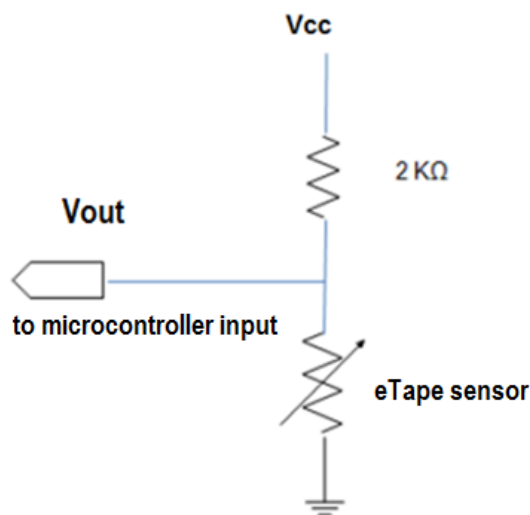


Figure 7. Voltage divider circuit with an eTape sensor

Figure 7 shows how eTape sensor installation on the network. At this circuit, the voltage is proportional to the resistance of the eTape sensor, thus :

$$V_{out} = [V_{cc} \times R_{eTape}] / [2K\Omega + R_{eTape}] \quad (2)$$

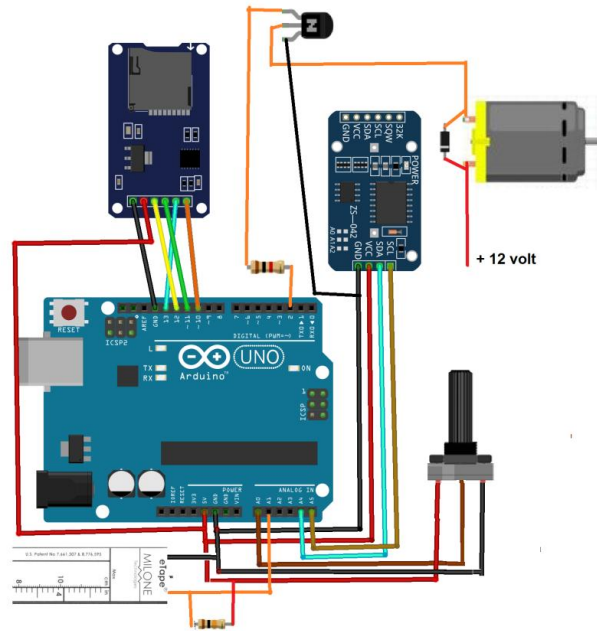


Figure 8. Water flow rate control and data acquisition circuit

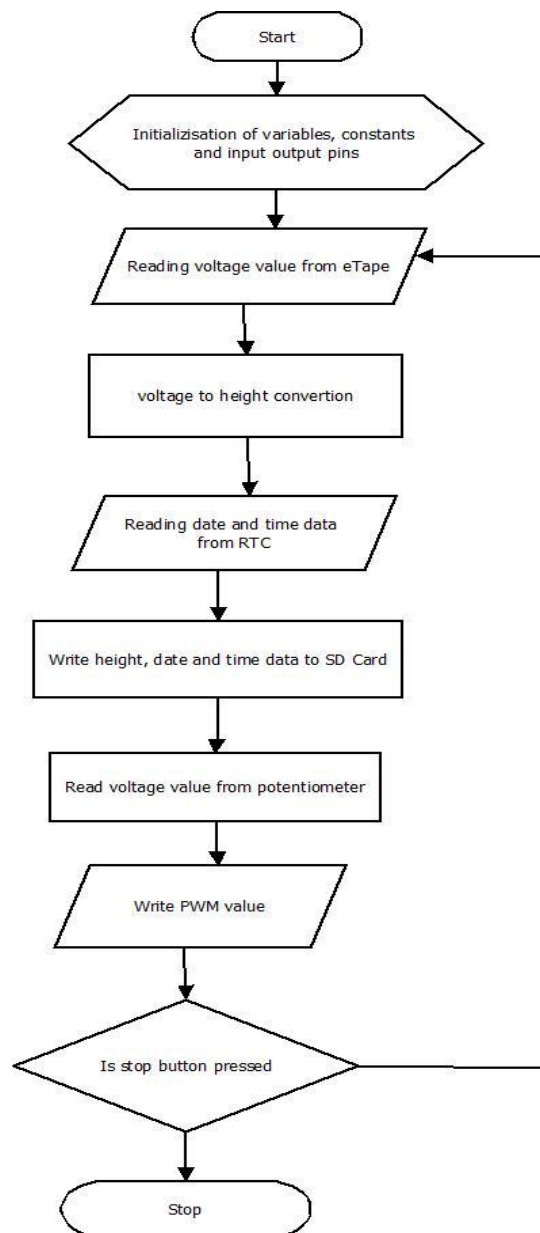


Figure 9. Flowchart of flow rate control

The electronic circuit for controlling water rate and data acquisition is shown in Figure 8. While the flow diagram of how the system works is shown in Figure 9.

4 Results and Discussion

The results achieved by this study are the completion of initial data retrieval. Model enhancements have also been made. The problem with the creation of a water rate

control model is the small motor torque at low speed. This is because the current entering the pump motor is still low while the voltage is reduced to reduce motor rotation. This problem causes the motor to not be strong enough to pump at low speeds so that small discharges are difficult to achieve. This problem can be overcome by adding obstacles to the suction hose. The obstacles used are cloth. The fabric resistance allows the pump to produce a small discharge at a rotation that is not too small.

The results of data retrieval using the model have shown results in accordance with the initial hypothesis. The results of data collection showed that the results of distillation water using the control of the water rate were higher than the model without control of the water rate. The results of data collection can be seen in Table 1.

Table 1. Distillation output and efficiency for various flow rate

Duration (Minutes)	Distillation output (kg)						Efficiency (%)					
	First flow rate 0,3 l/hour		First flow rate 0,5 l/hour		First flow rate 1,2 l/hour		First flow rate 0,3 l/hour		First flow rate 0,5 l/hour		First flow rate 1,2 l/hour	
	Control with Microtroller	Mechanical Control	Control with Microtroller	Mechanical Control	Control with Microtroller	Mechanical Control	Control with Microtroller	Mechanical Control	Control with Microtroller	Mechanical Control	Control with Microtroller	Mechanical Control
40	0.000	0.000	0.000	0.000	0.000	0.000	1%	0%	0%	0%	0%	0%
80	0.000	0.000	0.000	0.000	0.000	0.000	0%	0%	0%	0%	0%	0%
120	0.198	0.000	0.031	0.010	0.013	0.000	21%	0%	3%	1%	1%	0%
160	0.315	0.000	0.279	0.084	0.243	0.027	25%	0%	22%	7%	19%	2%
200	0.629	0.000	0.346	0.105	0.288	0.283	40%	0%	22%	7%	18%	18%
240	0.791	0.000	0.575	0.174	0.503	0.360	42%	0%	30%	9%	26%	19%
280	1.056	0.000	0.751	0.227	0.661	0.616	48%	0%	34%	10%	30%	28%
320	1.285	0.000	0.899	0.272	0.948	0.827	51%	0%	35%	11%	37%	33%
360	1.501	0.000	1.182	0.358	1.164	1.002	53%	0%	41%	12%	40%	35%
400	2.040	0.189	1.344	0.407	1.380	1.231	64%	6%	42%	13%	43%	39%
440	2.324	0.324	1.658	0.503	1.856	1.456	67%	9%	47%	14%	53%	42%
480	2.521	0.404	2.031	0.616	1.955	1.798	66%	11%	53%	16%	51%	47%

Figure 10 shows the results of distillation water at various water flow rates of 0.3 liters/hour. The water distillation model that uses a water flow rate controller with a microcontroller can produce far more distilled water. Up to minutes to 365 distillation models that use mechanical settings (taps) do not produce distilled water. This is due to the occurrence of problems in the mechanical flow settings. A common problem especially at small flow rates is the cessation of water flow that will enter the distillation model. The cessation of flow in the mechanical control, especially in small streams, is due to the presence of water vapor which clogs the canal.

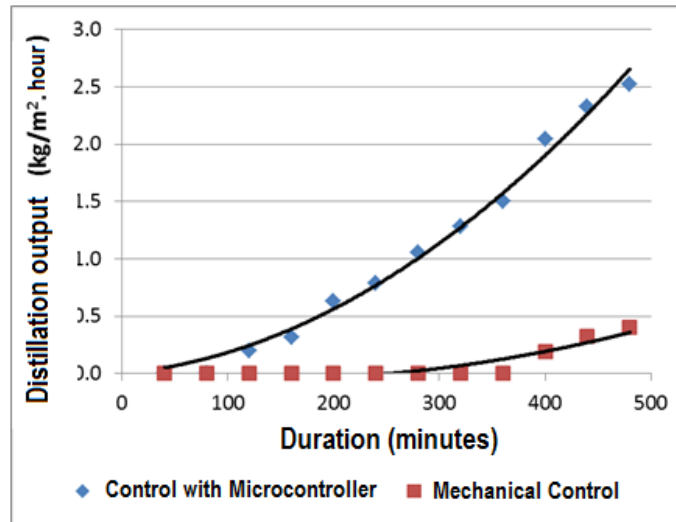


Figure 10. Comparison of distillation output at flow rate of 0,3 liter/hour

At the water flow rate of 0.5 liters/hour or in variation number 2 (Figure 11), the results of distilled water models with water flow rate controller using microcontroller is bigger than the distillation models without adjusting the flow rate with microcontroller or using mechanical controller (faucet). In contrast to variation number 1, it appears that a water distillation model with a mechanical control has produced distilled water in the 150th minute. This is because the water flow rate of distillation in variation number 2 is greater than variation number 1. At the higher water flow rate there is fewer problem compared with mechanical flow rate control at the smaller flow rate. The problem of mechanical control in variation number 2 is to reduce the water flow rate to the initial setting. The reduced flow is generally also caused by the appearance of water vapor which blocks the flow of water that will enter the distillation model.

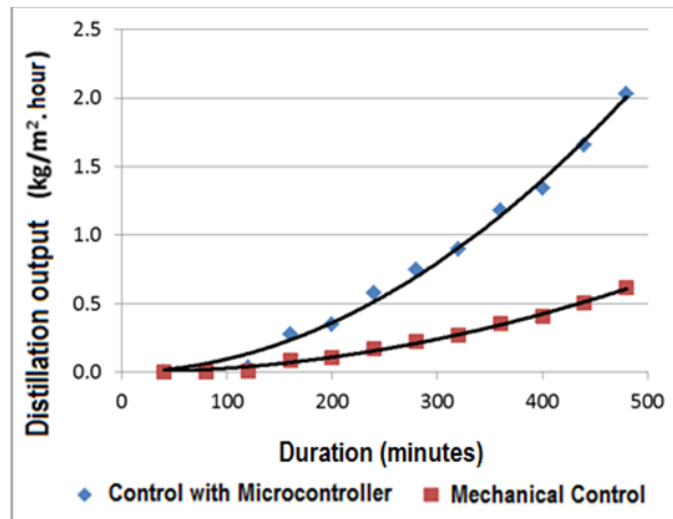


Figure 11. Comparison of distillation output at flow rate of 0,5 liter/hour

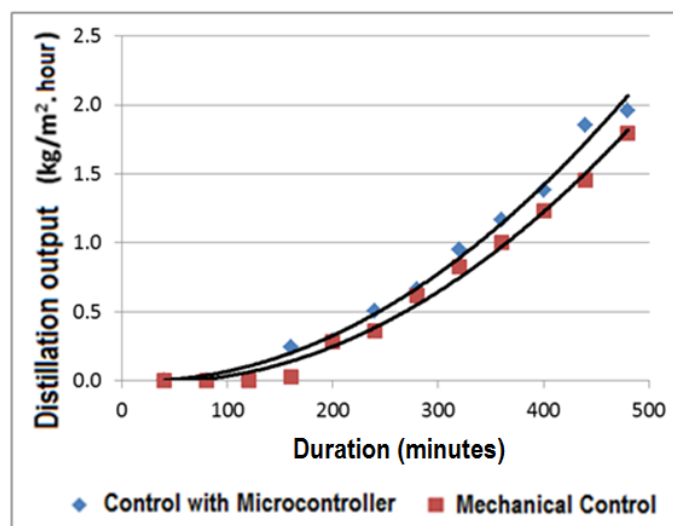


Figure 12. Comparison of distillation output at flow rate of 1,2 liter/hour

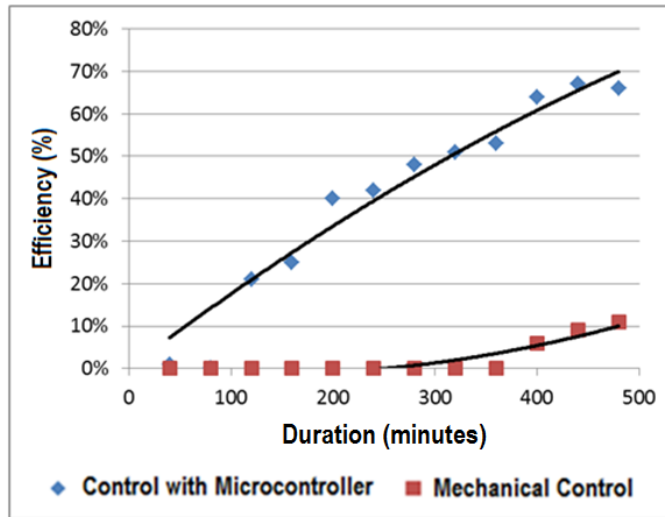


Figure 13. Efficiency comparison of a distillation model at flow rate of 0,3 liter/hour

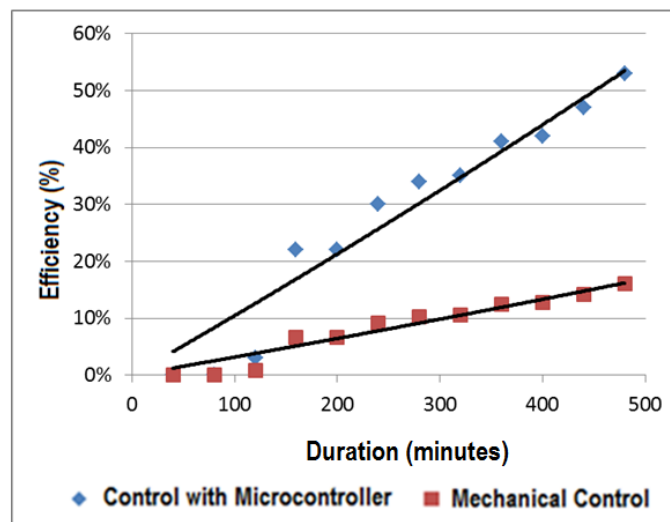


Figure 14. Efficiency comparison of a distillation model at flow rate of 0,5 liter/hour

In variation number 3 by setting the initial flow rate of 1.2 liters/hour it is seen that the distillation model with a mechanical arrangement begins to produce distilled water from the 90th minute (Figure 12). In variation number 3 the results of distillation of water models with microcontroller settings still produce more distilled water than the distillation model with mechanical settings. There is problem with mechanical control, when the water flow rate is large enough, the water flow rate increases from the initial

setting. This causes the evaporation process is not optimal so that the results of distillation water are also small.

The efficiency produced in the three variations shows a linear value with the results of distilled water produced by each variation. This can be seen from Figures 13, 14, and 15.

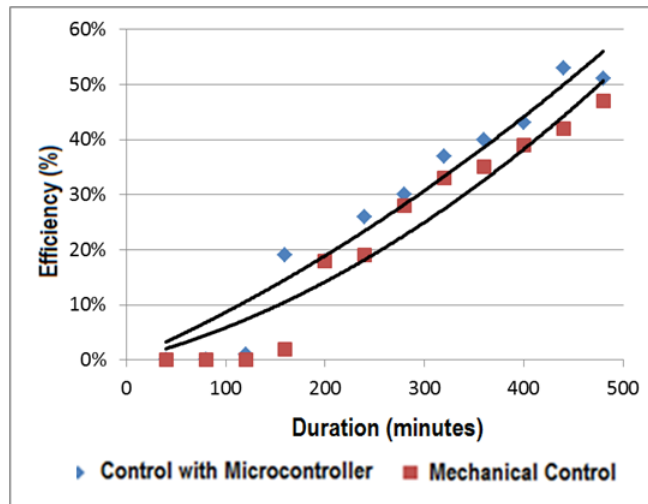


Figure 15. Efficiency comparison of a distillation model at flow rate of 1,2 liter/hour

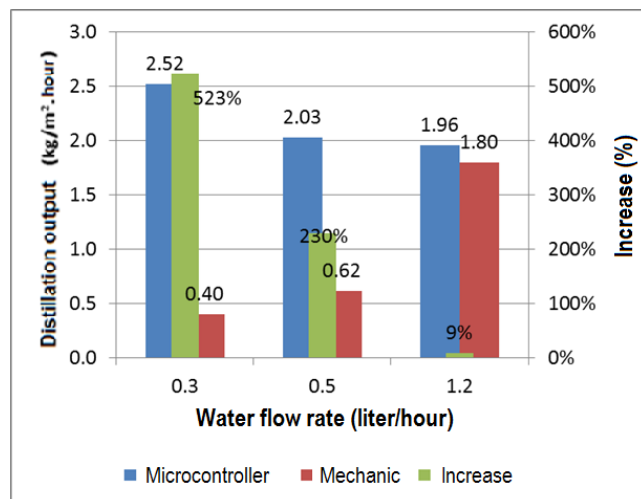


Figure 16. Comparison of distillation output at the flow rate of 0,3; 0,5 and 1,2 liter/hour

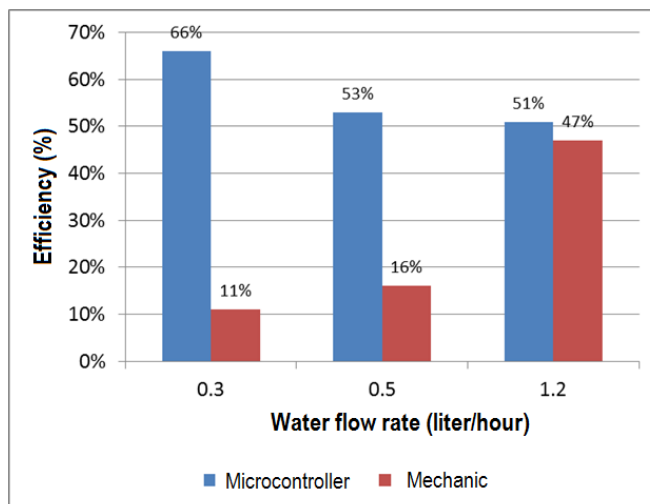


Figure 17. Efficiency comparison of distillation output at flow rate of 0,3; 0,5 and 1,2 liter/hour

In general, the increase in distillation water yield due to the use of microcontroller-based intake of water flow can be seen in Figure 16. The biggest increase in distillation water results with microcontroller-based water flow control compared to mechanical settings is 523%. The biggest increase occurs at the planned initial intake water flow of 0.3 liters/hour (water flow rate enter the smallest distillation). The highest efficiency produced by microcontroller-based distillation is 66% at a water flow rate of 0.3 liters/hour (Figure 17).

5 Conclusion

The conclusion that can be taken in general this research is that the results of distillation water using microcontroller-based water rate control is a maximum of 523% compared to the model sans water rate control 0.3 liters/hour, with distillation efficiency of 66%. From the results of this study it can also be concluded that microcontroller based water speed control is more stable than mechanical water flow control, especially in small flow.

Acknowledgements

This work would not have been possible without the financial support from DP2M DIKTI which has funded this *Penelitian Dosen Pemula* project. Thank you to the relevant parties in the process of conducting this research, DP2M DIKTI, Politeknik Mekatronika Sanata Dharma which have supported this research.

References

- [1] H. M. Ahmed, A. K. Al Taie, and M. Almea, “Solar water distillation with a cooling tube,” *International Renewable Energy Congress*, pages 6–10, November 2010.
- [2] T. J. Jansen, *Teknologi Rekayasa Surya*, PT Pradnya Paramita, Jakarta, 1995.
- [3] A. J. N. Khalifa and A. M. Hamood, “Experimental validation and enhancement of some solar still performance correlations,” *Desalination and Water Treatment*, **4** (1-3), 311–315, 2009.
- [4] D. W. Medugu and L. G. Ndatuwong, “Theoretical analysis of water distillation using solar still,” *International Journal of Physical Sciences*, **4** (11), 705–712, 2009.
- [5] M. Banzi and M. Shiloh, *Getting Started with Arduino: the Open Source Electronics Prototyping Platform*, Maker Media, Sebastopol, 2015.
- [6] M. W. Volk, *Pump Characteristics and Applications 2nd Edition*, CRC Press, Boca Raton, 2005.
- [7] G. Caraballo, “An arduino based control system for a brackish water desalination plant,” *Master Thesis*, University of North Texas, Denton, 2015.
- [8] N. Banerjee, S. Mukherjee, A. Mitra, A. Sanyal, and S.T Mandal, “Arduino based liquid dispensor system using peristaltic pump,” *B. S. Project*, West Bengal University of Technology, Kolkata, 2017.
- [9] <https://milonetech.com/p/about-etape> (Accessed on 25-05-2019).

Morphological Map Analysis in Design Cashew Sheller (*Kacip*) as a Creative Process to Produce Design Concept

Bertha Bintari Wahyujati

*Department of Mechatronics Product Design,
Politeknik Mekatronika Sanata Dharma, Yogyakarta, Indonesia
Corresponding Author: bertha.bintariwahyujati@gmail.com*

(Received 29-05-2019; Revised 17-10-2019; Accepted 17-10-2019)

Abstract

The design of cashew nut or cashew nut sheller uses appropriate or low technoshelly with consideration of low cost for tool material. This pengkacip tool will be used at Ngudi Koyo, Imogiri, Bantul, Yogyakarta. Cashew shell peeler or cipling device as a result of the design is a modification of the existing cashew shell peeler. Some parts of the existing tool are applied to several modified parts, namely the lever mechanism, picking knife, or lever knife. This paper will discuss the method of selecting a suppressor, lever and picking system on a tool using the morphological chart analysis method. Morphological charts will produce alternative designs for cashew nut peeler. The selection of alternative designs will be carried out by analyzing the results of testing in a technical mechanism, material strength, and alternative design quality values. Testing of alternative technical systems mechanisms is done by comparing the mechanical systems of existing tools. The size of the tool uses the anthropometric measurements of the female operator's body, because the operators in the Ngudi Koyo UKM are all women. The tool size adjustment

will provide to work more comfortable and increase efficiency. Quality testing in addition which is using standard anthropometric standards, will be tested for quality of ease to maintenance, ease to mobility, cleanability, neat, simple and safety tool.

Keywords: effective technoshelly, low technoshelly tool, security, design alternative testing

1 Introduction

UKM Ngudi Koyo Production System is a production that depends on supply and orders. Production cannot be carried out continuously because the supply of cashew nuts is not always in same quantity and quality, also because cashews only can be harvesting in October per year. These unstabil quantities cause the production have to be flexible in production system. Production depends on the order, availability of material and availability of time of the worker. The character of this production system causes production equipment not always to be operate. Equipment that not be operated will be stored in the UKM's production house, so the equipment needs are concise, do not require a big space and portable [1].

The production operators at Ngudi Koyo UKM are all farmers, so the cashew nut production business is a side business. As a side business, the production of cashew nuts is expected to be done on the free time when all farming work is completed done. The workers who are all woman work on the process of stripping the shell, stripping the epidermis and packing the cashews. Workmanship is often taken home because of the flexible work time and workmanship that can be taken to work other jobs at home. Therefore, a sheller that has easy to move places becomes a very important.

Flexibility also needed beside of the need of construction strength tools, including the possibility of working using this tool using their own table, easy to operate, and can be used at any time. Tools that have the capacity in accordance with the capabilities of each worker can be owned as a personal tool.

With the limitations of the specifications as needed for the cashew nut sheller, the design method that will be applied will be the analyzing method of morphological chart.

Morphological charts will facilitate selection of components in each part of the tool. Thus, after getting alternative designs, it will be analyzed to determine the best alternative choice for the design to be improved. The cashew nut sheller is expected to be used for small-scale production, empowering operators, improving the value in production of cashew nuts at UKM Ngudi Koyo.

2 Technical Data and Specifications of Cashew Nut

Spindles

Cashew nut is a fruit from Cashew tree. Cashew plant with the Latin name *Anacardium occidentale* L is a plant that lives in dry areas, and has little rainfall. The physical cashew fruit is a fake fruit as an enlargement of the fruit stalk. The fruit which is called as cashew nuts, located at the tip of the fruit. Cashew trees are filling plants between fields and villages of the villagers. One cashew tree can produce an average of about 1 quintal of cashew.

Cashew trees only have one harvest cycle season; in August, cashew trees start flowering, the process until the fruit ready for harvest is in October. Harvest cashew fruits are intended to harvest cashew nuts. The cashew nuts then will be dried under the sun rays for about one week. Drying the nuts intended for storing raw materials in production houses. Cashew nuts in perfect dried cashew can be stored for last more than a year. The production process is usually started before the holidays based on orders. The storage process will be important before the cashew through the next process, which is the separation of nuts from the shells using kacip.

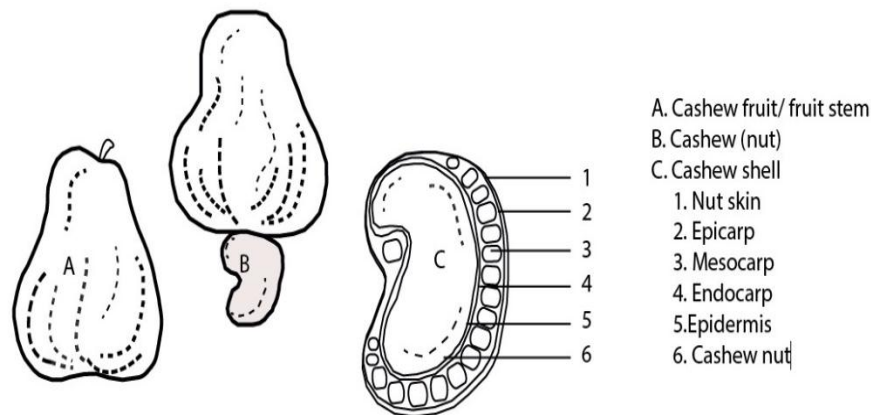


Figure 1. Cashew and its parts [2]

Cashew shells have hard skin called the Pericarp consisting of three layers, namely: the epicarp layer, the mesocarp layer, and the endocarp layer. Epicarp is the outermost skin, the outermost layer that has hard and tough properties. Mesocarp is the middle layer which has the thickest layer of the three layers of skin. In the Mesocarp layer there are conduits that drain liquid CNSL (Cashew Nut Shell Liquid) which are sticky and toxic. This liquid could irritate skin, and is toxic to be eaten. Endocarp is a soft inner layer [2]. These all are illustrated in Figure 1, where A shows cashew fruit, it is also a fruit stem, B shows cashew’s nut, and C shows cashew shell and its parts: 1. nut skin, 2. epicarp, 3. mesocarp, 4. endocarp, 5. epidermis, and 6. cashew nut.

Data of cashew shells measurements will be used to design the sheller include the average size of cashew shells, the depth of the skin that can be penetrated by the blade without breaking the cashew nuts, the speed of knife pressure, and the blade pressure to the cashew nut also the direction which is most effective to get the cashew nuts. Look at the Table 1 below:

Table 1. Results of measurement and weighing of weights of cashew nuts [2]

Criteria	A	B	C	D	E	F
Length (mm)	53,00	40,00	34,00	29,00	27,00	19,00
Width (mm)	32,00	33,00	22,00	20,00	19,00	14,00
Thickness (mm)	17,00	23,00	14,00	17,00	11,00	8,00
Weight (gr)	15,00	15,00	7,00	5,30	3,80	1,23

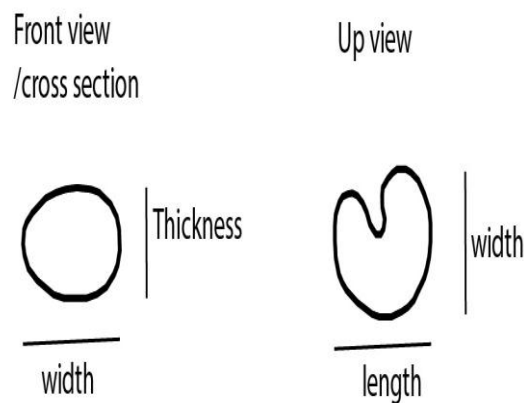


Figure 2. Position of measurement cashew shells [3]

The data is used to determine the optimal size for cashew nut clamp. The optimal size must be able to accommodate each size, so it must be considered a factor of flexibility to clamp different sizes of cashew. The use of a system presses towards the outer shell of the log to penetrate the maximum layer of the mesocarp, or the middle layer which is porous and contains liquid CNSL (Cashew Nut Shell Liquid). The data needed is about the average depth of the gelindong from the outermost layer of the skin to the middle layer, to determine the maximum depth of the knife piercing the cashew nut. The depth of the blade will determine the force used to press the piercing blade.

From the data it was found that the average cashew size was divided into 6 criteria for cashew nuts. The size of the clamp will be selected flexible clamp that can accommodate 6 types of cashew size. From the compressive velocity data and the average depth of the knife, a speed of 250 m/sec can be obtained which produces a 24 mm blade depth with a compressive force 4.84 N/m . This compression force will determine the type of spring and spring material to be used. In Table 2 and Table 3 we can see the speed of emphasis of cashew nut blades and relationship between the compressive force charged and size cashew nut. We can also see the position of compressing cashew logs in Figure 2. The data used to determine the optimal size for cashew nut clamp. The optimal size must be able to accommodate each size, so it must be considered the factor of flexibility to clamp different sizes of cashew. The use of a

system presses towards the outer shell of the shell to penetrate the maximum layer of the mesocarp, or the middle layer which is porous and contains liquid CNSL (Cashew Nut Shell Liquid). The average depth of the shell from the outermost layer of the skin to the middle layer, to determine the maximum depth of the knife piercing the cashew nut. The depth of the blade will determine the force used to press the piercing blade.

The cashew size was divided into 6 criteria for cashew nuts. The size of the clamp will be selected which can be flexible that can accommodate 6 types of cashew size. From the compressive velocity data and the average depth of the knife, a speed of 250 *m/sec* can be obtained which produces a 24 *mm* blade depth with a compressive force 4.84 *N/m*. This compression force will determine the type of spring and spring material to be used. Look at the Table 2 and Table 3 below:

Table 2. Speed of emphasis for the depth of cashew nut blades [2]

Press speed (m / sec)	Average knife depth (mm)	Press force
1.67	23,70	4,84
2.50	24,00	4,84
3.33	24,00	4,90

Table 3. Relationship between the compressive force charged (kgf) to the cashew nut and the size changes that occur [2]

No	Maximum load	Average compressive force (kgf)	Reduced size in shape (mm)
1.	Pressure on the thick side	48,40	4,70
2.	Pressure on the long side	64,70	11,30
3.	Pressure on width	49,20	7,80

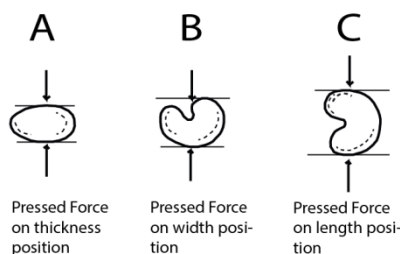


Figure 3. Position of compressing cashew logs [2]

Before get pressure from the knife, position of the cashew nut should be in the middle of the cashew nuts. It found in this position, the cashew are not too deformed due to pressure. Deformation of a pressure that is too large will cause the cashews be splitted because of knife pressure when piercing the shell. The position to get the optimal pressure and be able to open the shell is position B. The advantages of this position is because the shape of the cashew nut which has an inner basin in its shape. To open the shell without made nut be splitted, the tip of the blade must be shaped as a triangle to pierce the part of the cashew basin. Some positions of compressing cashew logs are shown in Figure 3.

The force of pressing the knife into the cashew nut will determine the shape of the blade tip chosen. The position of pressing the knife to pierce the cashew nut, and the position of the cashew nut against the blade horizontally or vertically will determine the amount of pressure on the blade given. The position of the cashew nut from its shape determines the size of the blade. The depth of the blade is determined by the maximum depth until the middle layer so that the blade shape should be tapered at the end. After the blade pierces the cashew nut then the blade is tilted as a lever end to separate the cashew nuts from the shell.

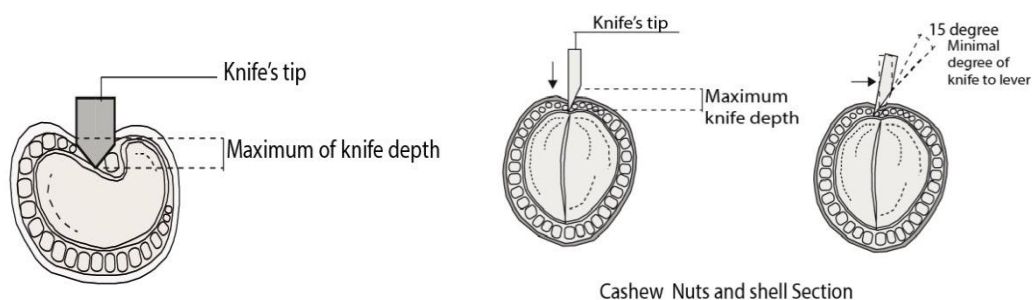


Figure 4. Maximum depth of blade

The slope of the blade is to leverage at a minimum of 15-20 degrees. The magnitude of the lever angle will affect the leverage or torque applied to the blade. Illustrations are given in Figure 4, where details are presented in Table 4.

Table 4. Relationship between Torque magnitude and torsional angle to release cashew nuts from the skin [2]

Size angle of suppressor (degree)	Average maximum torque (kgf.cm)
15	28,00
20	29,20
45	28,30

The production process at Ngudi Koyo UKM can not finish in one day process. Work carried out separately in each employee's house. The production process will be handling as separately works. Worker do the job at home to peeling the spindles, and the skin of the cashews.

Within 1 day, workers are usually able to peel cashew nuts as much as 7 kg of cashew nuts. The salary received by workers is *Rp. 7000/kg*. Cashew which has been peeled dried to make easier to stripping of epidermis. Cashews will be prepare as raw cashew nuts and fried cashews. Cashew nuts for raw orders will be dried before ready to be packaged. While the order of fried cashew nuts processed in frying process.

Raw cashew nuts will be divided into 3 quality criteria for cashew nuts based on customer orders, there are whole cashew nuts and split cashew nuts which will be packaged separated will be sell at price *Rp. 120000/ kg*. Meanwhile, crushed cashew nuts are sold at a price between *Rp. 60,000 – Rp. 80,000*. The sale of mixed cashew nuts consists of whole cashew nuts, split cashews and crushed cashew nuts sold at prices ranging from *Rp. 80000 to Rp. 90,000*.

Cashew nut sheller is called kacip. Kacip is a tool with a knife modified with a wooden frame, measuring 30 centimeters long. This kacip wood tool consists of a knife that has a wood and pressing knife blade. Cashew shell is placed under the blade inside the nut holder, the cashew nut is held with the thumb and forefinger. The position of the other fingers holds the cashew nut that has not been peeled. Stripping of the cashew nuts is by putting cashew nuts one by one. Stripping must be carefully because raw cashew has liquid sap which is very irritating. The selling price of whole cashew as good quality is higher, the stripping of cashew nut should not splitted into two parts. The cashew nut shelling equipment in recent time only owned by a few workers, because not everyone has the expertise to peel the cashew nut with good quality result.

3 Morphological Chart Analysis Method

The method of designing the cashew nut sheller is to mapping the part of the important part of the sheller based on the reference of the existing tool. The method of analyzing morphological maps is carried out by step-determining the technical criteria and mechanisms, material criteria, strength criteria, quality criteria. These criteria make it easy to set and sort the appropriate components. The level of criteria used for the whole tool is divided into parts. The parts of the tool are as follows: buffer construction parts, lever parts, knife parts, tool holder parts and cashew nuts. All parts of the tool are then given alternatives to then be combined into a concept of alternative tools. The alternative concept is then described thoroughly. Of all alternatives will be analyzed using an analysis of the criteria of technical specifications and mechanisms, the strength of the material and the quality determined based on the criteria of the specifications that are according to the needs of the tool.

4 Technical Criteria and Mechanisms

Technical analysis is a functional and technical analysis related to the mechanism for the peeler system. In addition, technical analysis covers the analysis of the structure construction of the constructor of the peeler [4].

4.1 Technical Specifications

The existing cashew sheller is called *kacip*. The tool is made of one blade with a slit in the side of the knife. Laying cashew logs one by one held with fingers without safety. Incorrect pressing of the knife causes the skin not to be peeled or the cashew split into two. Therefore not everyone can peel the cashew using *kacip*.

For the design of cashew nut sheller, use the *kacip* reference. Tools modified from frames that were previously made of wood, replaced with metal. The blade is replaced by using stainless steel. Stainless steel blade chosed because the material safe to use for food and food ingredients. The price of this material is more expensive than iron material. The knife is designed as a flat plate with the tip of a pointed triangle blade with an angle 15-20 degree. The type of knife edge we can see on Figure 5.

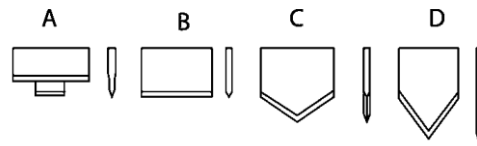


Figure 5. Type of knife edge

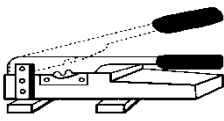
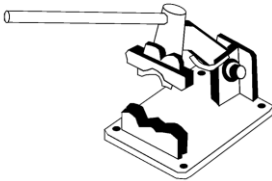
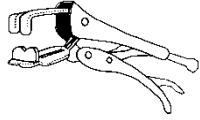
The lever system and presses on the blade use hinges that are retained with a spring. The place for laying cashew nuts uses a clamp system as a position guard. Placement of cashew remains one by one using a clamp that can be moved towards the blade. Difficulty in placement if done in large volumes poured because the shape of the cashew logs is not uniform, the size is different. The position of the cashew nut to be peeled must be on the back of the cashew nut. The directional lever system perpendicular to the direction of stabbing is intended to leverage the cashew seeds out of their shells. Lever knives use a maximum torque of 20 so that there is a minimum formed angle of 15 degrees.

Mohamad Saldin Wibowo (IPB, 2011) examined the size of local Indonesian cashews and obtained three lengths of cashew nut cashew fruit. The size is to determine the size of the blade to be used on the cashew nut peeler [5]. The blade is determined from the size of the cashew log data, namely 33 *mm* long blade for piercing large cashew logs (28.50 – 32.15 *mm*), 29 *mm* long blade for piercing medium sized cashew nuts (24.80 – 28.45 *mm*), 25 *mm* long blade for piercing small size cashew nuts (21.05 – 24.75 *mm*). The three types of knife sizes are taken; the average size is (29 *mm*) determining the size of the blade allows accommodating the piercing function of the three criteria for the size of the cashew logs.

4.2. Morphological Chart

The method of morphological maps requires comparison of tools from existing tools, judging by their weaknesses and strengths so that they can be used as new references and innovations [6]. Innovations in this regard cover modifications. We can see this at Table 5

Table 5. Analysis of existing tools

Tool Type			
Tool's name	<i>Kacip</i> (wooden sheller) The blade on the whole <i>kacip</i> is made to match	<i>Kacip</i> flat plate With this complete	<i>Kacip</i> ripper clamps The cashew coil is
Operational	the natural shape of the cashew nut so that the blade only splits the skin several millimeters thick as the skin is cut. After the skin is split, the cashew seeds are removed using a knife or flat nail	<i>kacip</i> , 8 kg of cashew nuts are obtained per person per day (one day 8 hours work) with a capacity of 70% whole seeds and 30% fractions consisting of halves, fragments, groats and dust	placed in the clamp gap then pressed like a hand-held motion
working deficiency	Cashew shell are placed one by one and held by hand, maybe the cashew is split very high, need trained people, cashew must still be gouged with other tools from the shell of the shell	Cashew shell are still placed one by one on a jagged base, still not safe	Cashew sponges are still placed one by one, the pressure must be careful, the possibility of lettuce and nuts split.

The analysis of work methods or functional analysis of the tools observed above, the lack of tools to find the best solution for modification so that it will be more optimal. The optimal standard results that are referenced are fewer split cashew nuts. In the functional analysis found similarities in the working principle, namely the first step is to stab cashew nuts and then pick out the cashew seeds. The design of the cashew nut peeler consists of the following sections

a. Supporting framework

The supporting frame is a frame that serves to support the entire cashew shelling unit. The supporting frame also serves to resist the forces that occur due to the transmission of force and the weight of the load.

b. Lever handle

The lever is an arm for channeling the pressure force and then leveres on the blade to stab and gouge the cashew nuts.

c. Spring

The spring can reduce vibrations due to the movement of the lever when stabbing and gouging the cashew nut shell. The position of the handle will return to its original position by using a spring after the lever is moved. The spring can be used to regulate and control the compressive force so that the distance of the blade press can be controlled to adjust to the cashew log posture to be peeled. The spring also functions to reduce the pressure applied by the operator.

d. Knife

This knife functions when the blade pierces the shell of the cashew nut and to bring it up to release the cashew nuts from the cashew seeds. The edge of the paring knife has a blade that has a 15 o tip and a smooth angle so that it can pierce the cashew nut. The tip of the pointed blade will be more in line with the size of the different cashew nuts, because it can pierce according to its posture. The tip of the pointed blade accommodates the shape of the cashew nut overdraft. This is so that the blade can pierce the skin at the desired position and depth so that the cashew seeds remain intact.

4.3. Ergonomic Analysis

Working comfort, the ease of operating tools and security when operating tools is an important criterias. Working comfort is determined by the compatibility between work position and tool size. Ease of operation in terms of the mechanism of the tool and ease of use, it is not complicated, easy to learn and use energy as lightly as possible. While the safety of work is viewed from safety against accidents caused by device errors, operator accident and equipment damage.

Ergonomics as one of the considerations for the design criteria for the design of the peeler is determined from the comfort side of the operator working while sitting, rarely hands when reaching, holding, rotating and security aspects against the danger of cutting [7].

The anthropometric data used with the data subjects were women aged 20 years - 47 years. The measured anthropometry is the female operator who works for the Ngudi Koyo UKM. From the measurements obtained anthropometric data as follows in Table 6 and Figure 6 :

Table 6. Anthropometric data of female workers [5]

No.	Body Dimension	5%(mm)	X(mm)	95%(mm)	SD
1	Eye Height	1279	1388	1497	66
2	Shoulder height	1130	1260	1389	79
3	Height of eye in sitting position	576	650	723	45
4	Shoulder height in a sitting position	462	515	569	33
5	Elbow height in a sitting position	161	186	211	15
6	Thigh thick	87	110	133	14
7	Distance from the buttocks to the knees	422	508	595	53
8	Distance from folding knees to buttocks	388	429	470	25
9	Knee height	417	458	499	25
10	Knee height	357	395	433	23
11	Pelvic width	282	328	374	28
12	Distance from elbow to fingertip	258	297	337	24
13	Front hand grip distance	543	596	649	32

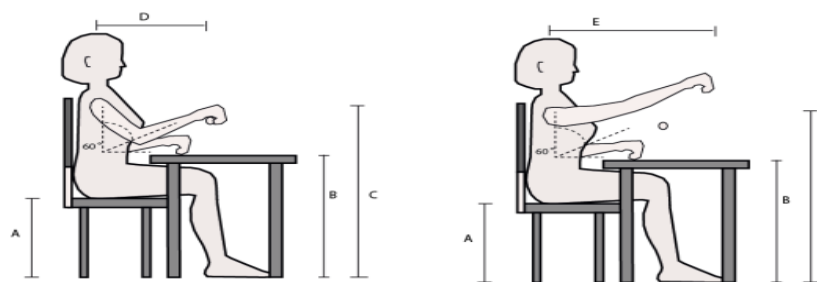


Figure 6. Normal arm reach and farthest arm reach

With calculations using body size from the data above, it is determined that the pengacip lever handle

- a. Size Height handle = Height of chair + Size of elbow height in sitting position + allowance

Dimensions: elbow height in sitting position, 50th percentile

Allowance: 50 *mm*

Calculation: $450 + 187 + 50 = 687 \text{ mm}$ (measured from the floor to the maximum height of the handle on the tool. The size obtained from the calculation is the normal height of the elbow in the sitting position plus the seat height. The maximum angle for the normal position of the arm is 90° . The calculation used 50th percentile or average value so that all operators can adjust properly.

b. The shortest distance for the handle range of the operator

Dimension: distance from elbow to fingertip

Calculation: $337 - 69 = 268 \text{ mm}$. The shortest distance of the handle range of the operator must not be smaller than the length of the forearm. In order to be accommodated by all operators, a 95th percentile is used as the minimum size

c. The farthest distance from the operator

The farthest distance from handle = length of fore *arm* + *y*

r = shoulder height in a sitting position elbow in a sitting position

y = $\sin 60^\circ = 300 \times 0.866 = 260 \text{ mm}$

Dimension = shoulder height at sitting position = 515 mm
(average value)

Elbow height at sitting position = 186 *mm*

Distance from elbow to finger tip = 297 *mm*

tip

Female finger length Percentile = 5

Calculation = $260 + 258 - 69 = 450 \text{ mm}$

The maximum distance reached so that percentile 5 is used so that the operator has it smaller extreme sizes could reach. The upper arm angle with body 60° because it is the angle for optimal attraction [8].

d. Handle diameter

Handle diameter according to Petrofsky, 1980 in Sritomo W, 2000 optimal size for women is a maximum of 4 *cm* – 5 *cm*.

5 Sketch Design for Modifying the Cashew Peeler

The method of morphological maps is used to find alternative concepts of the cashew tool design. Selection of alternatives is to choose an alternative concept that is closest to fulfilling the specifications of the tools needed. Mapping parts and components of the tool based on the concept of existing tools on the market. Alternative selection will also consider the criteria established as a reference for choosing alternatives.

Determination of the specifications of the tool is prepared from the needs of the user and identified from the problems in the process of working on the existing tool. Look at Table 7 below :


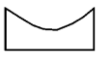
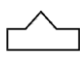

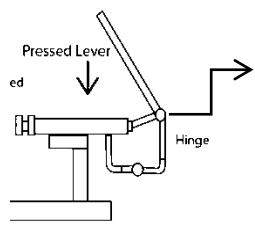
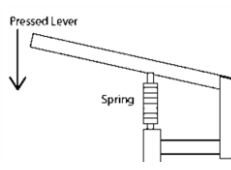
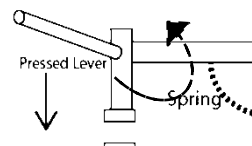
Table 7. Alternative analysis, morphology chart

No	Specifications	Category	Aspect	Code Specifications
1.	Cashew seeds separate from cashew nuts	D	Function	A1
2.	Cashew seeds are not split	D	Function	A2
3.	the safety of the fingers when peeling cashew is very important	W	Safety	B
4.	Power to peel as lightly as possible	W	Ease to operate	C1
5.	The sheller tool considers the position of work comfort (ergonomics)	D	Ergonomic	D1
6.	The weight of the pengacip tool is no more than 16 kg, as a limit to women's lifting ability	W	Ergonomic	D2
7.	Production tools are portable so they can be used anywhere	W	Ease to operate	C2
8.	The tool is easy to maintain, durable and strong.	W	Ease to maintenance	E

The latest design uses as reference tool, it is made as a morphological map to make it easier to analyze the components of the design of the tools. Analysis of morphological maps can be used to provide changes and modifications to the shortcomings of the tools used as references. Modification can be a total or partial change. The main need for modification is to meet the needs of users, both in the form of functions and aspects of criteria that are arranged as requirements for criteria or specifications. Modification is an innovation that is applied as an alternative design concept at Table 8.

Table 8. Analysis of alternative concepts, morphological charts

<p>Analyze alternative concepts from Reference</p>			
	<p>a.</p>	<p>b.</p>	<p>c.</p>
<p>1. Lever</p>			
	<p>The lever system uses a press hinge and rotates, the arm behind</p>	<p>Spring system 1/3 front arm</p>	<p>Rear spring system, lever to press on beside</p>
	<p>Operational lever angle elbow range $> 90^\circ$ maximum hand reach from the front</p>	<p>Operational lever angle elbow range $> 90^\circ$, maximum hand reach from the front</p>	<p>Operational lever angle elbow range $\leq 90^\circ$ hand reach $\leq 50\text{ cm}$ from the front</p>
<p>2. Pressing lever</p>			
	<p>Lever horizontally</p>	<p>Lever press vertically</p>	<p>Lever press vertically</p>
	<p>The press lever creates a thrust force in the cylinder pressing cylinder horizontally</p>	<p>Press lever creates a compressive force on the blade pressing lever vertically</p>	<p>Press lever creates a compressive force on the blade pressing lever vertically</p>
<p>3. Blade position and casing clamp holder</p>			
	<p>The clamp is in front and at the back, as a knife</p>	<p>The blade is at the top, the bottom becomes a clamp</p>	<p>The clamp is at the bottom, the knife is at the top</p>

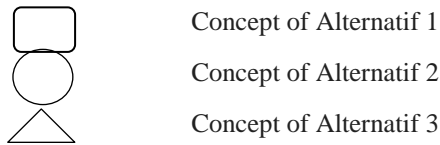
	Laying cashew is difficult because of the position above without restraint	Laying is easy but not safe, hands can be hit by a knife	Easy laying, hands can be hit by a knife
4. Blade shape		 	
5. Mechanism	The lever is pressed down then the lever will push the blade, then rotate the lever clockwise	The lever is pressed down, the hand position is more than 90°	The knife is pressed down using the right lever, the position of the arm can still be conditioned less than 90°
6. Material	Metal tube as a peel lever and press lever	Plate Bend	Combination of metal plate and metal tube
7. Joint Structure	The joint uses 2 hinges in the motion joint: 1 press motion hinge and 1 rotary motion hinge for 90°	Joint uses pin, spring, vibration and returns to its original position due to spring	Joint uses pin, spring, vibration and returns to its original position due to the spring, then moves to rotate the direction clockwise
			
	Using hinges, so that the compressive force requires energy to push the blade towards the cashew skin	Using the front spring, the position of the lever above makes it difficult for the hand to reach, but the pressure will be stronger, and more tiring	Using a spring on the back of the lever before the lever pin axle so that the compressive force is strong enough, the energy released is lighter, the angle of the hand is in the normal position.

8.	The operator is in direction of the maximum towards the tool	The operator is in front with the maximum straight range, the elbow angle is more than 90°	The operator is in front with the maximum straight range, the elbow angle is more than 90°	The operator is in front with a normal elbow
----	--	--	--	--

Arranging alternative concepts - alternative designs using a combination of components in the morphological map (see Table 9). Combinations are arranged based on the best possibilities so that they still allow the tool to function properly and meet the requirements of criteria and specifications wherever possible [6].

Table 9. Morphology chart

Notes for symbols in this Table:

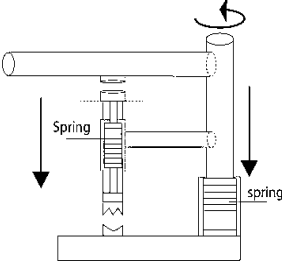
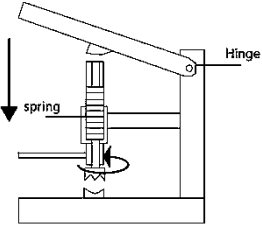
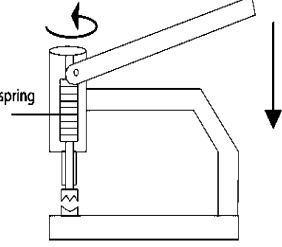


No.	Components	Option 1	Option 2	Option 3
1.	Lever	1a	1b	1c
2.	Pressing lever		2b	2c
3.	Blade position and cashing clamp holder	3a		3c
4.	Blade shape	4a		4c
5.	Mechanism		5b	5c
6.	Material	6a	6c	6c
7.	Joints structure		7b	7c
78.	The direction of the operator towards the tool		8b	8c
	Design new Concept Alternative 1	1a, 2b, 3c, 4c, 5c, 6a, 7c, 8b		
	Design new Concept Alternative 2	1b, 2c, 3c, 4a, 5b, 6b, 7c, 8b		
	Design new Concept Alternative 3	1c, 2b, 3a, 4c, 5b, 6c, 7b, 8c		

6 Results and Discussions of Design Concepts

The result of this study can be seen in Table 10 below:

Table 10. Analysis of alternative design sketches

No	Alternative	Component combination	Design sketch	Specification achievement
1.	Design new Concept Alternative 1	1a, 2b,3c,4c,5c,6a,7c,8b The concept of this tool uses two springs. The working system presses down with a spring, then rotates using a lever used to press the spring. Lever is in front of the operator		A1,A2,C1, D2,C2 5 criteria are met from 8 specification requirements
2.	Design new Concept Alternative 2	1b,2c, 3c,4a,5b,6b,7c,8b The concept of this tool uses one spring. The working system presses down with a spring, and then rotates using another lever on the blade body. Lever is in front of the operator.		A1,A2,C1, D2,C2,E 6 criteria are met from 8 specification requirements
3.	Design new Concept Alternative 3	1c,2b,3a,4c,5b,6c,7b,8c The concept of this tool uses one spring. The working system presses down with a spring, then rotates using a press lever The lever is the operator's farthest range from the front, but allows the operator to operate from the right side of the tool		A1,A2,B,C 1,D2,C2,E 7 criteria are met from 8 specification requirements

7 Conclusions

Analysis of alternative sketch drawings - alternative design concepts, is weighted which is judged by the fulfillment of the requirements of the criteria or specifications. The greater value indicates a tendency towards the selection of alternative design concepts. Improvements and improvements must still be made to the chosen design concept. In selected designs the most comfortable position is in front of the operator but normal hand reach with an angle should not exceed 90°. Thus the design change is

done by changing the handle direction to the side so that the handle range can be carried out in the normal position in Figure 7.

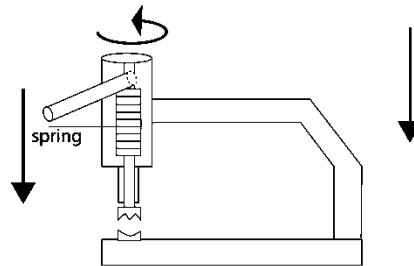


Figure 7. The draft concept was chosen as a peeler with a change in handle direction

The design of the cashew nut peeler is operated manually. The design of the tool size uses the anthropometric measurements of the female operator's body. Improvements in the comfort of work, namely by working in a sitting position, while the tool is placed on the work table. With the facing position from the front, at least the hands are better protected from the danger of being cut by a knife. The lever is located at the normal elbow position, so that the range meets ergonomic work comfort standards. Range of press levers. The way to operate this tool is to use the right hand to move the press lever, then the press lever is moved clockwise to help leverage the cashew seeds out of the cashew nut. The tool is protected with a cover that ensures safety, ease of cleaning and maintenance of the tool.

The weight of the tool is estimated by choosing the right material so that the weight of the tool becomes lighter. For the improvement of the design the next opportunity is the flexibility of the tool so that the tool can be adjusted to the work table and the seating position of all operators comfortably. With the concept of this tool design, the tool is expected to be easy to use and safe so that female workers at Ngudi Koyo UKM can work more effectively and efficiently.

References

- [1] Badan Pusat Statistik, *Kabupaten Bantul dalam Angka*, Badan Pusat Statistik Kabupaten Bantul, 2018.
- [2] Awaludin, Dace. *Modifikasi dan Uji Performansi Alat Pengupas Kulit Buah Mete*, Fakultas Teknologi Pertanian, Institut Pertanian Bogor, Bogor, 1995.
- [3] Direktorat Jendral Perkebunan, *Pedoman Pelaksanaan Pengembangan Jambu Mete*, Departemen Pertanian, Jakarta, 1979.
- [4] N. Cross, "Engineering Design Methods", *John Wiley & Sons*, Chichester, 2008.
- [5] M. S. Wibowo, *Modifikasi dan Uji Performansi Alat Pengupas Kulit Buah Mete Gelondong*, Departemen Teknik Mesin dan Biosistem, Fakultas Teknologi Pertanian, Institut Pertanian Bogor, Bogor, 2011.
- [6] E. Lutters, F. J.A.M. van Houten, A. Bernard, E. Mermoz, C. S. L. Schutte, "Tools and techniques for product design," *CIRP Annals*, **63** (2), 607– 630, 2014.
- [7] S. Ramadhan, Haniza, "Ergonomic facility design on station CV putra darma sorting," *Journal of Industrial and Manufacturing Engineering*, **1** (1), 46–55, 2017.
- [8] S. Wigjosobroto and Sutaji, "Analisa dan Redesain Stasiun Kerja Operasi Tenun secara Ergonomi untuk Meningkatkan Produktivitas," *Seminar Nasional Ergonomi, Teknik Industri FTI-ITS*, Surabaya. 2000.

This page intentionally left blank

Design and Development of a Path-Tracking System Based on Radio Frequency Identification Sensor for Educational Toy Robot (EDOT)

Martinus Bagus Wicaksono

*Department of Mechatronic Product Design,
Politeknik Mekatronika Sanata Dharma, Yogyakarta, Indonesia
Corresponding Author: baguswicax@yahoo.co.id*

(Received 31-01-2019; Revised 21-05-2019; Accepted 21-05-2019)

Abstract

This paper offers the design and development of a path-tracking system based on Radio Frequency Identification (RFID) sensors. This Path-tracking system will be used as a navigation system on EDOT. The EDOT requires a navigation system because it must be able to drive from the starting point to the predetermined end point automatically. This path-tracking system uses RFID sensors to detect RFID cards which have been arranged as a path. And then the EDOT will pass through the path consisting of some RFID cards. EDOT is a solution of a previous system, called Line-Follower, which uses infrared as a sensor to detect lines to guide a robot to go towards its destination point. The path-tracking system used by EDOT can work more efficiently in detecting the path to be traversed than other robots using the line follower system with infrared sensors or LDR (Light Dependent Resistor).

Keywords: path-tracking, RFID, EDOT, robot

1 Introduction

In recent years many children's toys have used robotic technology [1]. These toy robots are used to develop the ability of children, especially toddlers, to think logically. One of the technologies used is the line-follower robot, where the robot can go along the line that has been prepared beforehand.

In the game, the line as a robot guide when driving has been prepared first. This line is prepared so that it can guide the robot from one point (start point) to the destination point (endpoint). In general, the sensor used to detect the presence of lines is an infrared sensor. In fact, the performance of this sensor in detecting lines is strongly influenced by two things, namely the distance of the sensor to the line and the presence of external light. As well as in the game there are shapes and length of the track that cannot be changed according to the player's wishes. Thus the game will be limited by a number of things above.

This paper offers a design of a path-tracking system based on RFID sensors to detect RFID cards that have been arranged to form a path that the robot will pass. This system is more effective in reading paths that will be traversed by robots when compared to the line follower system that uses infrared sensors. In line follower that uses a light sensor (LED and Photodiode); the sensitivity of the sensor will be greatly influenced by the light around the robot [2]. Another line follower system that uses the LDR sensor as a tracking and navigating sensor on the robot also has almost the same recommendation, which is greatly influenced by the distance of the sensor to the detected line and also the reflection of light from the surrounding environment [3]. In other applications, the RFID sensor is used to detect the identity of the car that will enter the parking area and provide information on the parking position of the car [4]. For the path-tracking system using the RFID sensor, it will use a standard RFID sensor on the market. As well as the RFID card that will be used as a robot track compiler, it will use a standard RFID card on the market. This system will use the Arduino Nano as a control system. All needed components will use standard components on the market to reduce prices and accelerate the process of making a Path-tracking system.

This paper is written in the following structure: in part 2 it will describe the design of the path-tracking system on EDOT. The method of making Path-tracking system will be described in section 3. While the results of the research and discussion will be written in section 4.

2 Design

In this section, we explain about the design of our proposed system. RFID sensors are sensors that use radio wave-based technology. This sensor will detect objects called RFID cards. The communication method of these two objects is with the RFID sensor emitting waves that will trigger the power and clock on the RFID card to send data in the form of the identity that has been written on the RFID card.

In this design the RFID card will be used and arranged as a path, RFID sensors that will be used to detect trajectories, Arduino Nano as a control system, DC motor driver used as a motor movement regulator, the DC geared motor is used as the main movements generator of the robot. The block diagram representing the process is shown in the figure 1 below. This path-tracking system is designed using standard components on the market. The purpose is to simplify the replacement of components if damage occurs due to misuse. Another reason is that components on the market will be cheaper compared to customized components.



Figure 1. Block Diagram of the path tracking system

In some applications, RFID cards are used to store personal identity data. And in the existing system the card will be used for student attendance detector [5]. In this design, RFID path-tracking system, the path will use some RFID cards that have been given a different identity according to the required command, as shown in table 1. The cards are RFID card 125 KHz as shown in the figure 2 below.

Table 1. List of RFID card identity

No	Card identity	Command
1	0000001990	Forward
2	0000002350	Turn left
3	0000002357	Turn right
4	0000002334	Stop

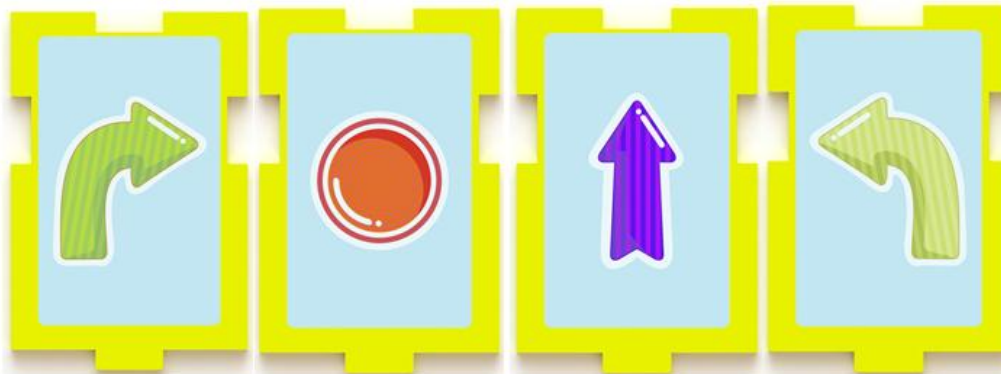


Figure 2. RFID card: turn right, Stop, Forward, Turn Left

The RFID Sensor RC522, as shown in Figure 3, is used to detect the RFID cards which have their own identity. The sensor is installed at the bottom of the robot, so that it can directly detect the RFID card which is arranged as the path that EDOT will pass. The position of the sensor is placed between the main wheels to make the EDOT move easier along the pre-arranged track.



Figure 3. RFID Sensor

A microcontroller, Arduino Nano, is used to control EDOT based on reading data on an RFID card carried out by an RFID sensor. The program has been written on a

microcontroller that will control the rate of EDOT following the prepared path. Data received by the RFID sensor which is the result of reading the RFID card will be an input to the microcontroller. The microcontroller will send the command to the DC motor driver which will adjust the rotation of the DC motor as the main driver of the EDOT as shown in Figure 4.

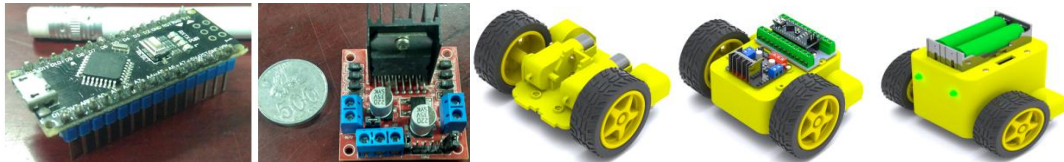


Figure 4. Arduino Nano, DC Motor Driver (L298N), part of EDOT

Figure 5 shows the overall shape of EDOT that uses the RFID sensor as a path-tracking system. As discussed in the previous paragraph, the RFID sensor is placed on the bottom surface of the EDOT facing the track. This is so that the sensor can detect the track properly. Figure 6 shows EDOT is moving following the prepared path. RFID cards must be arranged so that they give the same direction as the arrows on the RFID card.

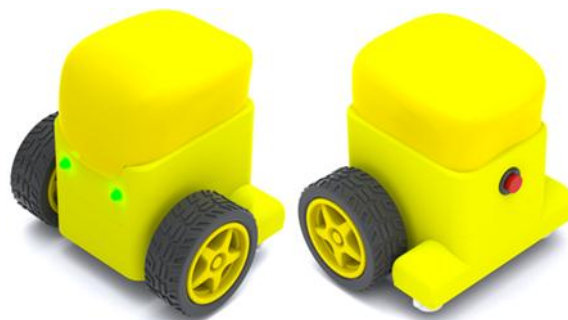


Figure 5. The EDOT

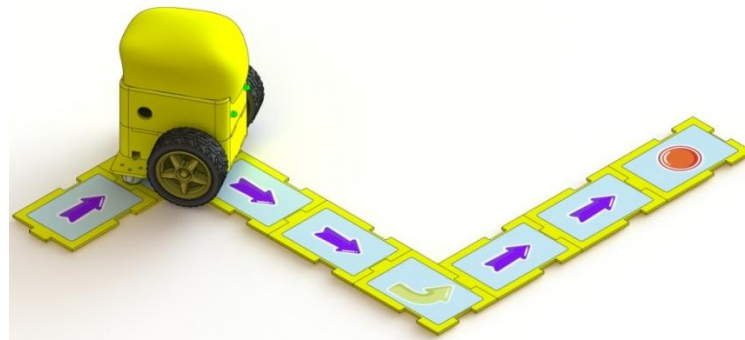


Figure 6. EDOT on the Path

3 Method

This section is devoted for the research method. In order to validate the system, some experiments in path-tracking have been conducted. The purpose of the experiments is to know the responses of the system in tracking a path. Some RFID cards with different identities were used to check the system accuracy in detecting the path. The procedure of the experiment is as follows:

1. Set the identity of some RFID cards based on the command (forward, turn left, turn right, stop),
2. Make 5 cards in every command,
3. Run the path-tracking system,
4. Detect the RFID card,
5. Vary the distance of the sensor to the card, and
6. Record the observations of the system.

By detecting the different card and varying the distance of the sensor to the card, the data in table 2 to table 7 could be obtained.

Table 2. Detection distance of 1 mm

No	Type of command	Detection Result
1	Forward	Success
2	Turn Left	Success
3	Turn Right	Success
4	Stop	Success

Table 3. Detection distance of 10 mm

No	Type of command	Detection Result
1	Forward	Success
2	Turn Left	Success
3	Turn Right	Success
4	Stop	Success

Table 4. Detection distance of 20 mm

No	Type of command	Detection Result
1	Forward	Success
2	Turn Left	Success
3	Turn Right	Success
4	Stop	Success

Table 6. Detection distance of 25 mm

No	Type of command	Detection Result
1	Forward	Fail
2	Turn Left	Fail
3	Turn Right	Fail
4	Stop	Fail

Table 5. Detection distance of 23 mm

No	Type of command	Detection Result
1	Forward	Fail
2	Turn Left	Fail
3	Turn Right	Success
4	Stop	Fail

Table 7. Detection distance of 30 mm

No	Type of command	Detection Result
1	Forward	Fail
2	Turn Left	Fail
3	Turn Right	Fail
4	Stop	Fail

To validate the system, it is tested in actual working conditions. The system will be used to read RFID cards that have been arranged in such a way as to form the path that will be traversed by EDOT. The purpose of this test is to get the right delay in reading the RFID card and sending the command for EDOT to move according to the identity of the RFID card before reading the next card that has been arranged to form the path that EDOT will pass. The data shown in table 8 to table 12 below.

Table 8. Time Delay of 3 seconds

No	Order of the cards	Result
1	F - F - F - S	Fail
2	F - TR - F - S	Fail
3	F - TR - TL - F - S	Fail
4	F - TL - TR - S	Fail

Table 9. Time Delay of 1 second

No	Order of the cards	Result
1	F - F - F - S	Fail
2	F - TR - F - S	Fail
3	F - TR - TL - F - S	Fail
4	F - TL - TR - S	Fail

Table 10. Time Delay of 0.75 second

No	Order of the cards	Result
1	F - F - F - S	Fail
2	F - TR - F - S	Fail
3	F - TR - TL - F - S	Fail
4	F - TL - TR - S	Fail

Table 11. Time Delay of 0.5 second

No	Order of the cards	Result
1	F - F - F - S	Success
2	F - TR - F - S	Success
3	F - TL - F - S	Success
4	F - TL - TR - F - S	Fail

Table 12. Time Delay of 0.3 second

No	Order of the cards	Result
1	F - F - F - S	Fail
2	F - TR - F - S	Fail
3	F - TR - TL - F - S	Fail
4	F - TL - TR - S	Fail

Abbreviation		
F	:	Forward
TR	:	Turn Right
TL	:	Turn Left
S	:	Stop

4 Results and Discussion

We shall present our research results and discussion in this section. The experiment data in table 2 to table 4 indicate that no error occur in path detecting process. Meanwhile, the experiment data in table 5 up to table 7 indicate that error occur in path detecting process. Since there is no problem with Arduino program, it is highly possible that the errors are mainly from the hardware configuration. The maximum detection distance is below 23 *mm*. The performance of the path-tracking system can be improved by setting the RFID sensor distance to the RFID card in between 1 *mm* up to 20 *mm*. The rigidity of the structure is also important to be taken into account for better result.

In the validation test, as we can see in the table 11 that the result of the test gives the best performance when the time delay was set to 0.5 second. Although in the fourth experiment it was not successful. There are several causes for this failure, such as the friction between the surface of the wheel and the trajectory, the thickness of the card that interfere the EDOT movement, etc.

From a number of experiments that have been carried out to produce conditions where the position of the RFID sensor must be installed at a distance of less than 23 *mm* from the surface of the track. Another parameter is setting the time delay. This will be used to adjust the time duration of the wheel to move after the sensor detects the track. The best delay time is around 0.5 seconds to get accurate results in reading RFID cards by RFID Sensors.

5 Conclusion

Design and development of a path-tracking system based on Radio Frequency Identification sensor for the Educational Toy Robot(EDOT) have been discussed in this paper. The path-tracking system has been tested by detecting the RFID cards in various distances and different command as well as by using real track out of arranged RFID cards. Based on data, some error still occurs in detecting processes. However, the source of the errors has been identified to be followed up. Improving the detecting quality of the path-tracking system may become the future research.

References

- [1] G. A. Demetriou, “Mobile robotics in education and research,” in *Mobile robots: Current trends*, Z. Gacovski, Ed. Croatia: InTech, 27–48, 2011.
- [2] D. A. N. Janis, D. Pang, and J. O. Wuwung, “Rancang bangun robot pengantar makanan line follower,” *Jurnal Teknik Elektro dan Komputer*, **3** (1), 1–10, 2014.
- [3] Y. Prabowo and S. Hepy, “Line follower robot berbasis mikrokontroler ATMEL 16,” *Jurnal Ilmiah BIT*, **8** (2) 44–52, 2011.
- [4] F. A. Imbiri, N. Taryana, and D. Nataliana, “Implementasi sistem perparkiran otomatis dengan menentukan posisi parkir berbasis RFID,” *ELKOMIKA: Jurnal Teknik Energi Elektrik, Teknik Telekomunikasi, & Teknik Elektronika*, **4** (1), 31–46, 2016.
- [5] N. Sparkhojayev and S. Guvercin, “Attendance control system based on RFID-technology,” *IJCSI International Journal of Computer Science Issues*, **9** (3), 227–230, 2012.

This page intentionally left blank

Designing Independent Automatic Drinking Water Platforms at Sanata Dharma University

Muhammad Prayadi Sulistyanto^{*}, Ervan Erry Pramesta

Politeknik Makatronika Sanata Dharma, Yogyakarta, Indonesia

**Corresponding Author: prayadi.sulistyanto@gmail.com*

(Received 23-01-2019; Revised 31-10-2019; Accepted 04-11-2019)

Abstract

Environmental pollution is increasing every year. From 2011 to 2014, environmental pollution in the Special Region of Yogyakarta increased above 250%. The effect of environmental pollution is the decreasing availability of clean water. Sanata Dharma University as an institution engaged in the field of education seeks to provide clean water where clean water is suitable for drinking, namely with RO (Reverse Osmosis) technology. Drinking water distribution has run well in Sanata Dharma University, but it lacks hygiene. In this study, researchers Designing Independent Automatic Drinking Water Platforms that could distribute clean water ready to drink for students with a certain dose. The result of this study is that an independent automatic drinking water platform can provide 200 cc of clean water ready for drinking in 9 seconds each time a user (student) uses this tool.

Keywords: RO, drinking water platform, automatic water

1 Introduction

The level of environmental pollution in the Special Region of Yogyakarta, increased above 250 *percent* over the period of 2011 to 2014. The most common pollution in 2014 was air pollution, which occurred in 415 villages, while water pollution occurred in 44 villages and soil pollution occurs in 4 villages [1]. Environmental pollution is increasing every year, it will be inversely proportional to the need for clean water which continues to increase, so that it is obeyed by PT AQUA to open clean water plants, namely in the area of Klaten. Coinciding with World Water Day, the Klaten AQUA Factory held the inauguration of Embung Tirtamulya located in Pucang, Tegalmulyo Village, Kemalang District, Klaten to support water availability in a number of villages on the slopes of Merapi [2].

Various types of research related to efforts to reduce environmental pollution such as those conducted by Novita Sekarwati who conducted a study to reduce phosphate levels in laundry waste in the Tambakbayan, Catur tunggal, Depok, Sleman, Yogyakarta [3]. Another researcher, Oki Oktami Yuda, also conducted a study to suppress environmental pollution by controlling the pollution of hotel wastewater in the city of Yogyakarta in 2017 [4].

Sanata Dharma University, Yogyakarta, Indonesia as an institution engaged in the field of Education also strives to provide clean water where clean water is suitable for drinking, namely with RO technology. Drinking water distribution has run well in Sanata Dharma University, but it lacks hygiene in the supply of drinking water that is ready for consumption. So it takes a tool that can remove water cleanly, higinies and is able to remove water with the right dose and automatically.

This paper is written in the following structure. Part 2 describes the design of the tool. The method (steps) for making the tool will be described in Section 3. The results of the research and discussion are written in Section 4. This paper concludes with some conclusions.

2 Design

The components used are a *BJ300 – DDT – P* sensor, a 12 Volt in out ½ "Solenoid Valve, a 12 V Switch Adjustable Timer Switch Relay, and a 5 – foot 12 V Relay. *BJ300 – DDT – P* sensor is a sensor used to detect the presence of objects in front of it with a maximum detection distance of 300mm with the output type of this sensor being PNP [5]. Timer Switch Relay Adjustable 12V module is a tool to set the lag time to turn on / off the equipment with a time lag of 0 – 10 seconds. If you want a longer pause, you can replace the larger elco (C1). Can be applied to alarms, time lags on/off lights and others according to creativity [6]. In this study, the electrical circuit used is as follows in Figure 1.

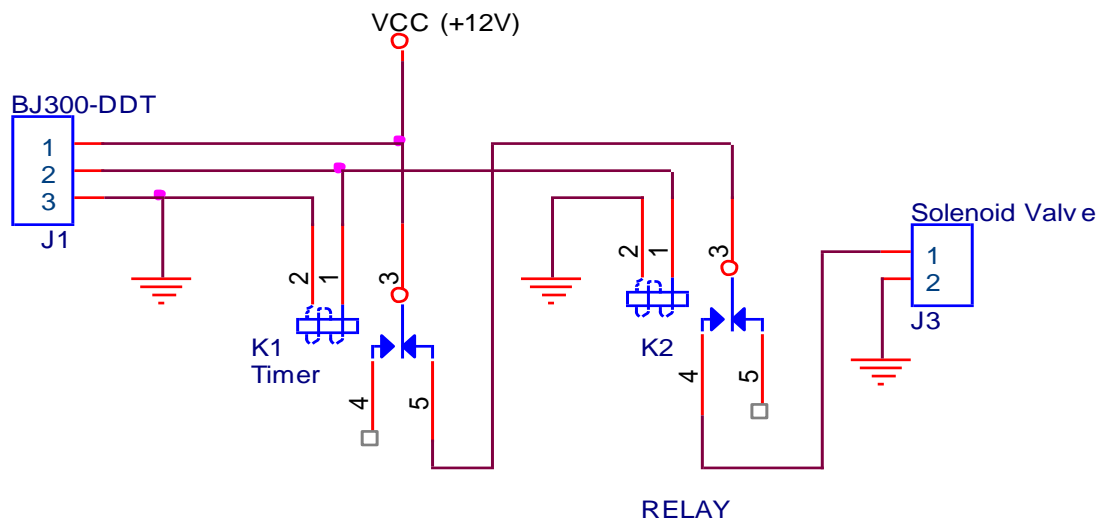


Figure 1. Electric Independent Automatic Drinking Water Platform

In Figure 1 the circuit used is quite simple, using only 5 components which are arranged in such a way that they can produce results according to the purpose of this study. The essence of the automated platform is the control of the opening of the faucet (solenoid valve) so that RO water can be distributed with a certain dose. The workings of the independent automatic drinking water platform system are as follows:

- a. Users (students) take a glass that has been provided, then bring it to the RO head and the presence of the hand will automatically be detected by the sensor *BJ300 – DDT*.

- b. The active sensor will activate the timer, and simultaneously activate the solenoid valve and because the solenoid valve is active, RO water will flow into the glass.
- c. The active timer will count at a certain time, and if the specified time has been reached, the solenoid will die and the RO water will stop flowing.
- d. RO water will still stop flowing even though the hand still reads the *BJ300 – DDT* sensor.
- e. RO water will also stop flowing when the hand is not read by the *BJ300 – DDT* sensor even though the timer has reached the specified time.

Independent automatic drinking water platform is designed so that the users feel aesthetically comfortable. Figure 2 shows a design drawing of 3 dimensions of independent automatic drinking water platform and Figure 3 shows the dimensions of the tools and parts of an independent automatic drinking water platform.



Figure 2. Design of an Independent Automatic Drinking Water Platform

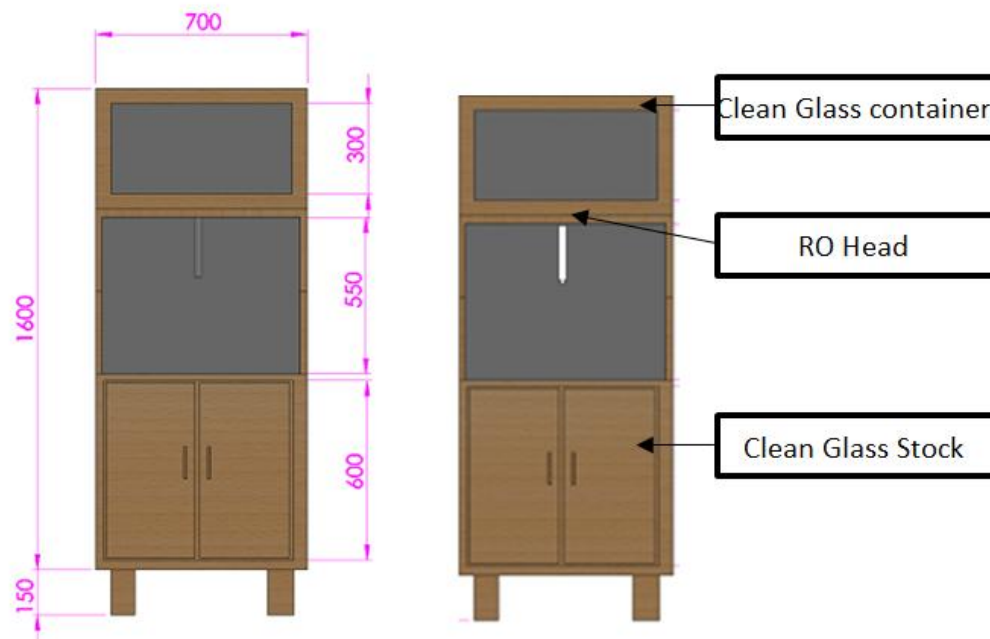


Figure 3. Dimensions and parts of the Independent Automatic Drinking Water Platform

The independent automatic drinking water platform designed has been equipped with a clean glass container that is ready to use which is above the RO head, making it easier for users to take advantage of this RO drinking water service. This tool is also equipped with a lower cupboard that can be used to store clean glass stock.

3 Method

The course of the research on the Design of an Independent Automatic Drinking Water Platform of Sanata Dharma University is:

a. Literature Review

Literature review is a study related to previous research and collects references *BJ300 – DDT – P*, Solenoid Electric Water Valve 12v Nc In Out 1/2 "Electric Faucet, New DC 12V. Pull Delay Timer Switch Relay Adjustable Module and material related to this research.

b. Making hardware

Making hardware starts from the design of placement of adapters, valves and sensors so as to facilitate maintenance.

c. Data collection

Data retrieval is done by doing a timer test on the amount of RO water that comes out so that later can be determined the right time to produce the volume of RO water as expected.

d. Conclusion

Conclusions are the final results that refer to the research objectives.

4 Results and Discussion

The results of the implementation of the design an independent drinking water platform are shown in Figure 4. Installation of the sensor under the spot where the glass is clean and the direction of the reading is directed to the end of the RO head so that the sensor can detect the glass at the end of the RO head.



Figure 4. Independent Automatic Drinking Water Platform of Sanata Dharma University at Campus III Paingan, Maguwoharjo, Depok, Sleman, Yogyakarta, Indonesia

Testing the system of independent automatic drinking water platforms is carried out with a source RO water discharge of 1.5 L/min. The test is done three times with the same timer value and monitors the RO water output that comes out.

Table 1. The first Test Result of the Independent Automatic Drinking Water Platform

Timer Value	Amount Of Water That Comes Out
1 second	–
2 second	4 cc
3 second	20 cc
4 second	32 cc
5 second	55 cc
6 second	90 cc
7 second	120 cc
8 second	165 cc
9 second	205 cc
10 second	260 cc

Table 2. Test Result of both Independent Automatic Drinking Water Platforms

Timer Value	Amount Of Water That Comes Out
1 second	–
2 second	5 cc
3 second	15 cc
4 second	28 cc
5 second	60 cc
6 second	95 cc
7 second	130 cc
8 second	160 cc
9 second	190 cc
10 second	250 cc

Table 3. Test Results Table of the Independent Automatic Drinking Water Platform

Timer Value	Amount Of Water That Comes Out
1 second	–
2 second	5 cc
3 second	15 cc
4 second	30 cc
5 second	60 cc
6 second	90 cc
7 second	130 cc
8 second	170 cc
9 second	200 cc
10 second	250 cc

The results of the tests carried out on an independent automatic drinking water platform, when the sensor detects and the timer is set to 1 second, RO water has not had time to flow as shown in Tables 1-3. This is because there are 3 components (2 relays and 1 solenoid valve) which is active based on the principle of magnetic induction, so that when the timer setting is given 1 second, the solenoid valve is only active for a moment and RO water has not been able to flow.

The next time setting is a multiple of 1 second and the test results get varied results. Increasing the amount of RO water volume every second gets different results in each test. RO Water Discharge the output of an independent automatic drinking water platform in the first 3 seconds is 5.55 cc/second . In the next second, the 4 to 6 seconds, the discharge of the RO water output from the independent automatic drinking water platform is 25 cc/second . In the next second, which is 7 to 9 seconds, the RO water discharge from the independent automatic drinking water platform is 35.55 cc/second .

The conclusion obtained from the research is that the RO water discharge from the independent automatic drinking water platform every second increases. The first 3 seconds to 9 seconds experienced a significant increase, up 30 cc/second . So to get 200 cc results, it only takes 9 seconds as shown in Tables 1-3.

5 Conclusion

The conclusions that can be drawn from the study entitled designing independent automatic drinking water platforms can distribute clean water ready to drink students with a certain dose well. Independent automatic drinking water platform are arranged with a timer with an ON time of 9 seconds, so that when the user (student) needs clean drinking water, just take the glass provided, and when the hand is detected by the sensor, the water will come out during 9 seconds at a rate of 200 cc . When the hand is not detected by the sensor, the water will automatically stop flowing even though the timer has not reached 9 seconds.

Acknowledgements

This research was financially supported by Sanata Dharma Foundation. The author thanks the Director of Politeknik Makatronika Sanata Dharma and Innovation Center Politeknik Mekatronika Sanata Dharma for some discussions.

References

- [1] L. Kertopati, *Pencemaran Lingkungan di Yogyakarta Meningkat 250 Persen*, <https://www.cnnindonesia.com/nasional/20161023224728-20-167372/pencemaran-lingkungan-di-yogyakarta-meningkat-250-persen> (Accessed on 23-01-2019,15:03 WIB).
- [2] <https://aqua.co.id/pabrik-aqua-klaten-resmikan-embung-tirtamulya-untuk-dukung-ketersediaan-air-bersih>, (Accessed on 23-01-2019,15:40).
- [3] N. Sekarwati, “Penurunan Kadar Total Phosphat (Po₄) pada Limbah Laundry dengan Metode Aerasi-Filtrasi Di Dusun Tambakbayan Catur Tunggal, Depok, Sleman, Yogyakarta”, *Jurnal Kesehatan Masyarakat*, **11** (1), 2018.
- [4] O. O. Yuda and E. P. Purnomo, “Implementasi Kebijakan Pengendalian Pencemaran Limbah Cair Hotel di Kota Yogyakarta Tahun 2017”, *Jurnal Administrasi Publik: Public Administration Journal*, **8** (2), 2018.
- [5] http://www.autoniconline.com/product/product&product_id=701 (Accessed on 24-01-2019,18:00 WIB).
- [6] New DC 12V Pull Delay Timer NE555 Switch Relay Adjustable Module, <https://www.tokopedia.com/solarperfect/new-dc-12v-pull-delay-timer-ne555-switch-relay-adjustable-module> (Accessed on 23-01-2019,19:10 WIB).

This page intentionally left blank

AUTHOR GUIDELINES

Author guidelines are available at the journal website:

<http://e-journal.usd.ac.id/index.php/IJASST/about/submissions#authorGuidelines>